Variations and sources of volatile organic compounds (VOCs) in urban region: insights from measurements on a tall tower

Xiao-Bing Li[1,2], Bin Yuan[1,2,*], Sihang Wang[1,2], Chunlin Wang[3,4], Jing Lan[3,4], Zhijie Liu[1,2], Yongxin Song[1,2], Xianjun He[1,2], Yibo Huangfu[1,2], Chenglei Pei[5,6,7,8], Peng Cheng[9], Suxia Yang[1,2], Jipeng Qi[1,2], Caihong Wu[1,2], Shan Huang[1,2], Yingchang You[1,2], Ming Chang[1,2], Huadan Zheng[10], Wenda Yang[9], Xuemei Wang[1,2], and Min Shao[1,2]

[1] Institute for Environmental and Climate Research, Jinan University, Guangzhou 511443, China

[2] Guangdong-Hongkong-Macau Joint Laboratory of Collaborative Innovation for Environmental Quality, Guangzhou 511443, China

[3] Guangzhou Climate and Agrometeorology Center, Guangzhou, 511430, China

[4] Southern Marine Science and Engineering Guangdong Laboratory (Zhuhai), Zhuhai, 519082, China

[5] State Key Laboratory of Organic Geochemistry and Guangdong Key Laboratory of Environmental Protection and Resources Utilization, Guangzhou Institute of Geochemistry, Chinese Academy of Sciences, Guangzhou 510640, China

[6] CAS Center for Excellence in Deep Earth Science, Guangzhou, 510640, China

[7] University of Chinese Academy of Sciences, Beijing 100049, China

[8] Guangzhou Ecological and Environmental Monitoring Center of Guangdong Province, Guangzhou 510060, China

[9] Institute of Mass Spectrometer and Atmospheric Environment, Jinan University, Guangzhou 510632, Guangdong, China

[10] Guangdong Provincial Key Laboratory of Optical Fiber Sensing and Communications, and Department of Optoelectronic Engineering, Jinan University, Guangzhou, 510632, China

[*] Corresponding authors: byuan@jnu.edu.cn

Abstract

Volatile organic compounds (VOCs) are key precursors of ozone and particulate matter, which are the two dominant air pollutants in urban environments. However, compositions and sources of VOCs in urban air aloft were rarely reported so far. To address this matter, highly time-resolved measurements of VOCs were made by proton-transfer-reaction time-of-flight mass spectrometer (PTR-ToF-MS) at a 450-m platform on the Canton Tower in Guangzhou, China. A combination of *in-situ* measurements and modeling techniques was used to characterize variations and sources of VOCs. Five sources were identified from positive matrix factorization (PMF) analysis, namely daytime-mixed (e.g., biogenic emissions and secondary formation), visitor-related (e.g., human breath, cooking, and volatilization of ethanol-containing products), vehicular+industrial, regional transport, and volatile chemical product (VCP)-dominated (i.e., volatilization of personal care products), contributing on average to 21%, 30%, 28%, 10%, and 11% of total VOCs (TVOC) mixing ratios, respectively. We observe that contributions of the visitor-related source, mainly composed of ethanol, followed well with the variation in visitor numbers on the tower. The VCP-dominated source only had an average contribution of ~5.7 ppb during the campaign, accounting for a small fraction (11%) of TVOC mixing ratios but a large fraction (22%) of the total OH reactivity. However, large fractions of reactive VOC species, e.g., monoterpenes (49%), were attributed to the VCP-dominated source, indicating important contributions of VCPs to ambient concentrations of these species in urban environments. Vertical profiles of air pollutants (namely NOx, ozone, Ox, and $PM_{2.5}$), measured at 5 m, 118 m, 168 m, and 488 m, exhibited more evident gradients at night than in the daytime owing to the stronger stability of the nocturnal boundary layer. Mixing ratios of VOC species during the nighttime generally decreased with time when the 450-m platform was located in the nocturnal residual layer and markedly increased when impacted by emissions at ground. The results in this study demonstrated composition

54 characteristics and sources of VOCs in urban air aloft, which could provide valuable
55 implications in making control strategies of VOCs and secondary air pollutants.

1 Introduction

Volatile organic compounds (VOCs) are important trace gases in the atmosphere and are composed of myriad chemical species (Pallavi et al., 2019; Wang et al., 2020a; Gkatzelis et al., 2021). Except for their direct adverse impacts on human health (Zhang et al., 2013), VOCs are also important precursors of secondary pollutants such as ozone and secondary aerosol (Vo et al., 2018; Zhou et al., 2019; Qin et al., 2021). Reduction in ambient VOCs concentrations is the key for synergistic control of both ozone and particle pollution. However, it is highly challenging for this target due to complex sources and chemical transformations of VOCs in urban environments (Yuan et al., 2012; Mo et al., 2016; Zhu et al., 2019).

In addition to compiling accurate emission inventories (bottom-up method) (Zheng et al., 2013; An et al., 2021), the combination of *in-situ* measurements and receptor models (top-down method) was widely adopted to quantitatively apportion sources of ambient VOCs (Baudic et al., 2016; Liu et al., 2016; Fan et al., 2021; Pernov et al., 2021). Concentrations of various VOC species can be measured by offline and online techniques. Gas chromatography-flame ionization detector/mass spectrometry (GC-FID/MS) combined with stainless steel canisters are the most popular offline technique (Guo et al., 2011; Yuan et al., 2013; Zhang et al., 2013; Qin et al., 2021). Automated online GC-FID system and high time resolution mass spectrometer, such as proton-transfer-reaction mass spectrometer (PTR-MS) and chemical ionization mass spectrometer (CIMS), are popular online techniques (de Gouw and Warneke, 2007; Wang et al., 2020a; Wang et al., 2020c; Fan et al., 2021; Ye et al., 2021). However, VOCs measurements made by both online and offline instruments are markedly affected by very local emission sources, particularly in urban environments, when they are usually deployed at ground level. This is highly important for studies aiming to characterize variations and sources of ambient VOCs at large spatial scales (such as a city or city clusters) based on measurements of only one site. To address this concern,

VOCs measurements made in the upper part of the planetary boundary layer (PBL) may be a better choice due to the well mixing of surface emissions when being transported upward from sources to observation sites (Hu et al., 2015a; Hu et al., 2015b; Squires et al., 2020).

As reported in the literature, *in-situ* measurements of VOCs at high altitudes (e.g., hundreds of meters or several kilometers above ground level) were predominantly made using the combination of offline techniques and samples collected by various platforms such as aircrafts (Geng et al., 2009; Xue et al., 2011; Benish et al., 2020), tethered balloons (Zhang et al., 2018; Wu et al., 2020b; Wang et al., 2021; Wu et al., 2021), high buildings and towers (Ting et al., 2008; Mo et al., 2020), and unmanned aerial vehicles (UAVs) (Vo et al., 2018; Liu et al., 2021). These offline measurements were predominantly used to reveal vertical variations of VOCs concentrations, impacts of VOCs degradation chemistry on the formation of secondary pollutants, and source characteristics of the species of interest. Offline measurements made at high altitudes were generally not capable of fully characterizing temporal variations of concentrations and source characteristics of VOCs due to strict limitations in their time resolution and sample sizes. In this condition, online VOCs measurements with fast response at high altitudes are required. Lack of available platforms has been a key limited factor for conducting online VOCs measurements at high altitudes in China. For instance, the combined utilization of aircraft and online spectrometer (such as PTR-MS) has been widely used in North America to measure VOCs concentrations in the lower troposphere (Hornbrook et al., 2011; Müller et al., 2016; Yuan et al., 2016; Koss et al., 2017; Fry et al., 2018; Chen et al., 2019), while it is quite difficult in China due to the lack of professional research aircraft and the strict control of airspace. Tethered balloons and UAVs are generally not suitable for online VOCs measurements due to their limited payloads (Dieu Hien et al., 2019). Tower-based platforms provide another path for online VOCs measurements at high altitudes in urban environments. However, tower-based online measurements of VOCs were only reported in Beijing, China so far

(Squires et al., 2020; Zhang et al., 2020).

In this study, continuous online VOCs measurements, including more than 200 species with a time resolution of 10 s, were made at a 450-m platform on the Canton Tower in the Pearl River Delta (PRD) region, China during August–November 2020. A combination of the VOCs measurements and the positive matrix factorization (PMF) receptor model was used to provide new insights into the concentrations, temporal variations, and source contributions of VOCs in urban region.

2 Methods and materials

2.1 Site description and field campaign

The PRD region is one of the most developed city clusters in China with more than 70 million residents by 2020 and is suffering from air pollution problems (e.g., ozone and secondary aerosol) (Wang et al., 2017; Wang et al., 2020b; Yan et al., 2020; Li et al., 2022). In this study, VOCs measurements were made at the Canton Tower (CTT, 23.11°N, 113.33°E) in Guangzhou, a large city in PRD (Figure S1), from August 18 to November 5 in 2020. The CTT has a total height of 610 m including the shaft on the top (Figure S1(c)). The observation was conducted in a room (Figure S1) at the 450-m Look Out platform (Jin et al., 2022), which is a ramp with stairs and is located on the top of the main body of the CTT. The observation room is located below the ramp and a sampling port is reserved on the wall outside the tower. A louver is located ~3 m below the sampling port. The 450-m Look Out platform is a famous tourist attraction with an opening time of local time (LT, UTC+8) 10:00–22:30, and visitors could walk around for a panorama of downtown Guangzhou. On each day, there are two busiest tourist hours, roughly at LT 11:00–14:00 and 18:00–21:00, on the 450-m platform. In addition, there are three restaurants between 376 and 423 m. The VOCs measurements were interrupted during October 8–12 due to instrument malfunction.

2.2 VOCs measurements

VOCs measurements were made using a high-resolution proton-transfer-reaction quadrupole interface time-of-flight mass spectrometer (PTR-QiToF-MS, Ionicon Analytik, Innsbruck, Austria) with both hydronium ion (H_3O^+) (Yuan et al., 2017; Wu et al., 2020a) and nitric oxide ion (NO^+) chemistry (Wang et al., 2020a). The H_3O^+ and NO^+ modes were automatically switched with 22 min for the H_3O^+ mode and 12 min for the NO^+ mode during the campaign. In this study, only VOCs measurements made in the H_3O^+ mode were used for analysis. In H_3O^+ mode, the PTR-QiToF-MS was operated with a drift tube pressure of 3.8 mbar, a drift tube temperature of 120 ℃, and a drift tube voltage of 760 V, resulting in an E/N (E refers to electric field and N refers to number density of buffer gas in the drift tube) value of ~120 Td (Townsend). Raw data of PTR-ToF-MS were processed and analyzed using Tofware software (Tofwerk AG, v3.0.3) and please refer to our previous works (Wang et al., 2020a; Wu et al., 2020a) for more details. Signals of 3035 ions with *m*/*z* up to 510 were obtained at time resolutions of 10 s. To measure VOCs concentrations outside the tower, a ~5 m long Perfluoroalkoxy (PFA) Teflon tubing (OD: 1/4") was used to connect the inlet of the instrument and the sampling port (Figure S1). The PFA Teflon tubing has been proven to be effective in measuring ambient concentrations of VOCs (Deming et al., 2019; Liu et al., 2019) and has been widely used in field studies (de Gouw et al., 2003a; Hu et al., 2011; Wu et al., 2020a). Air sample in the tubing was drawn by a pump at a flow rate of ~5 L min^{-1}. Blank measurements were performed automatically at the last 2 min of the H_3O^+ mode by passing ambient air through a platinum catalyst heated to 365 ℃.

A gas standard with 35 VOC species (Table S1) was used for calibrations of the PTR-ToF-MS once per day. Ten organic acids and nitrogen-containing VOC species were calibrated using a liquid calibration unit in the laboratory. Sensitivities of the remaining VOC species were determined using the quantification method based on reaction kinetics of the PTR-ToF-MS (Wu et al., 2020a; He et al., 2022). Impacts of the change in ambient humidity on measured signals of the PTR-ToF-MS were removed

using humidity-dependence curves of VOC species determined in the laboratory (Wang et al., 2020a; Wu et al., 2020a). The limit of detection (LOD) for a VOC species was defined as the concentration when the signal-to-noise ratio (SNR) equals to 3 (Yuan et al., 2017). Average mixing ratios, LODs, sensitivities, chemical formula, and suggested compounds of 225 VOC species used in this study are summarized in Table S1.

2.3 Other measurements

During the CTT campaign, a CO_2 and H_2O Gas Analyzer (Model: Li-840A, Licor Inc., USA) was deployed to measure carbon dioxide (CO_2, ppm in dry air) and humidity (mmol mol^{-1}). In addition, four air quality automatic monitoring stations are located at ground level (~5 m), 118 m, 168 m, and 488 m of the CTT, which report hourly concentrations of ozone, NO, NO_2, NOx, and $PM_{2.5}$ along with meteorological parameters, namely temperature (T), relatively humidity (RH), and pressure (Mo et al., 2020). Mass concentrations of gaseous pollutants were reported at 25 ℃ and 1013.25 hPa and were converted to mixing ratios (ppb) accordingly. Contour plots of vertical profiles of NOx, ozone, Ox (O_3+NO_2), and $PM_{2.5}$ concentrations were made using the bilinear method in Igor software (v8.04). Linear interpolations for concentrations of these pollutants were performed on both spatial (altitude) and temporal scales. A ceilometer (CL31, Vaisala, Finland) deployed on the Panyu Campus of Jinan University (23.02°N, 113.41°E, Figure S1), approximately 13.5 km to the southeast of the CTT, was used to measure planetary boundary layer height (PBLH) during the camapign. In addition, measurements of VOCs and CO_2 made on the campus of Guangzhou Institute of Geochemistry (GIG), Chinese Academy of Sciences (23.15°N, 113.36°E, ~25 m above ground level) during September–November 2018 (Wang et al., 2020a; Wang et al., 2020c; Wu et al., 2020a) were used for comparison with those measured on the CTT. *p* values were obtained using the Student's t-test to determine statistical significance levels of differences. The GIG site is located approximately 5.7 km to the northeast of the CTT. Measurements of VOCs and CO_2 at the GIG site were made using the same instruments as those at the CTT site.

2.4 PMF receptor model

The PMF receptor model was used to quantitatively analyze sources of the VOCs measurements made at the 450-m platform. The PMF model has been widely used to determine source contributions of measured VOCs concentrations in previous studies (Yuan et al., 2012; Pallavi et al., 2019; Pernov et al., 2021). A simple description of the PMF model was provided in the Supplementary Information (SI).

The PMF model was performed on 225 VOC species (Table S1) in this study. In preparation of PMF input data, measured concentrations of a VOC species below the LOD were replaced with half of the LOD and corresponding uncertainties were assigned to 5/6 of the LOD. Missing samples of a VOC species were replaced with its median value during the campaign and corresponding uncertainties were set as values equal to three times the median value (Zhang et al., 2013; Pernov et al., 2021; Qin et al., 2021). During the CTT campaign, the measured ethanol concentrations were impacted by the change in the number of visitors (a detailed discussion in Section 3.3) and exhibited strong variations (Figure 1). Thus, measurement uncertainties of ethanol calculated by Eq. (S3) were reduced by a factor of 5 to increase its weight in PMF analysis, which successfully resolved factors representing visitor influences and reduce residuals of PMF solution from over 20% to ~14%. The PMF analysis was performed using the PMF Evaluation Tool (v3.05) with Igor Pro (Ulbrich et al., 2009).

3 Results and discussion

3.1 Overview of field measurements during the campaign

As shown in Figure 1, concentrations of various species and meteorological parameters all exhibited strong variations during the campaign. Daily mean ozone mixing ratios varied in the range of 17.8–105.0 ppb with an average (± standard deviation) of 55.1 ± 18.3 ppb. Daily mean total VOCs (TVOC) mixing ratios, including a total of 225 species, varied between 23.9–124.2 ppb with an average of 62.1 ± 21.8 ppb. Daily mean NOx mixing ratios varied in the range of 7.9–31.6 ppb with an average

of 13.6 ± 3.8 ppb. Measured CO_2 mixing ratios exhibited strong variability with daily mean values ranging from 403.5 to 471.4 ppm. Ethanol was the most abundant VOC species, accounting on average for 23.5% of measured TVOC mixing ratios. Daily mean ethanol mixing ratios varied between 4.3–53.4 ppb with an average of 15.3 ± 9.1 ppb. Toluene was the most abundant aromatic species and had an average mixing ratio of 1.4 ± 0.9 ppb. Daily mean temperatures varied in the range of 17.7–29.0 ℃ with an average of 23.2 ± 3.0 ℃. Daily mean RH varied between 39.3%–85.0% with an average of 71.6% ± 10.3%. In general, the observation site was predominantly influenced by hot and moist air masses from August 18 to October 4, but cooler and dryer air masses from October 5 to November 5.

The most abundant 10 VOC species measured by PTR-ToF-MS during the CTT campaign were ethanol, methanol, acetic acid, formaldehyde, acetone, ethyl acetate, acetaldehyde, hydroxyacetone+propionic acid, toluene, and C8 aromatics, contributing to over 70% of TVOC mixing ratios. As shown in Figure 2, the 225 VOC species were classified into six categories, namely C_xH_y (i.e., hydrocarbons), $C_xH_yO_1$ (i.e., VOC species containing one oxygen atom), $C_xH_yO_2$ (i.e., VOC species containing two oxygen atoms), $C_xH_yO_{\geq 3}$ (i.e., VOC species containing three or more oxygen atoms), N/S containing species (i.e., VOC species containing nitrogen or sulfur atoms), and siloxanes (Wu et al., 2020a; He et al., 2022). The most abundant category was $C_xH_yO_1$, which had an average contribution of 67% to TVOC mixing ratios, but only contributed to 40% of total OH reactivity. The $C_xH_yO_2$ and $C_xH_yO_{\geq 3}$ categories contributed to 22% and 1% of TVOC mixing ratios, respectively. C_xH_y only accounted for 9% of TVOC mixing ratios but contributed to 37% of the total OH reactivity, indicating more reactive VOC species in this category. Concentrations of N/S containing species and siloxanes were generally lower than 0.5 ppb and totally contributed to ~1% of TVOC mixing ratios.

At ground level, each VOCs category accounted for comparable fractions in TVOC mixing ratios and the total OH reactivity to those measured at 450 m. However,

247 the majority of the C_xH_y, $C_xH_yO_{\geq 3}$, and N/S containing species measured at 450 m had
248 lower mixing ratios than those measured at ground level (Figures 2(b) and S2),
249 implying their predominant contributions from surface emission sources. Most of the
250 $C_xH_yO_1$ and $C_xH_yO_2$ species measured at 450 m had comparable mixing ratios to those
251 measured at the ground level. However, mixing ratios of some $C_xH_yO_2$, $C_xH_yO_{\geq 3}$, and
252 N/S containing species measured at 450 m were higher than those measured at ground
253 level, which can be attributable to either enhancement of their emissions on the 450-m
254 platform or more secondary formation from oxidation of VOCs (e.g., C_xH_y and $C_xH_yO_1$
255 species). The differences in contributions of VOCs categories to the total concentrations
256 and OH reactivity imply that sources of the VOCs measurements made at 450 m and
257 the ground level are different.

258 ## 3.2 Diurnal variations in selected VOC species

259 Average diurnal profiles of nine selected VOC species measured by PTR-ToF-MS
260 during the CTT campaign are demonstrated in Figure 3. Measurement results at GIG in
261 2018 are also shown for comparison to investigate differences in their diurnal variation
262 patterns and likely sources. In addition, average diurnal profiles of the selected VOC
263 species on working and non-working days (including weekends and public holidays
264 when the 450-m platform had more visitors) during the CTT campaign are compared
265 to explore potential emissions from visitors. Average diurnal variations in ratios of
266 concentrations of selected VOC species measured on non-working days to those
267 measured on working days were also calculated, as shown in Figure S3. Meteorological
268 factors, namely temperature and RH, exhibited insignificant differences between
269 working and non-working days (Figure S4). Thus, the differences in VOCs
270 concentrations between working and non-working days were not notably impacted by
271 the change in meteorological conditions.

272 Diurnal profiles of aromatic species, including benzene, toluene, and C8 aromatics
273 measured at 450 m exhibited similar variability with minima occurring between LT
274 12:00–16:00. Aromatics with higher chemical reactivity could be removed more rapidly

by reactions with hydroxyl radicals (OH) in the daytime (Yuan et al., 2012; Wu et al., 2020a). In addition, rapid elevation of the daytime PBL could enhance the dilution of chemical species, leading to rapid decreases in their concentrations (Sangiorgi et al., 2011; Zhang et al., 2018). The two effects are the two most important factors for controlling diurnal profiles of aromatics measured at 450 m. By contrast, diurnal profiles of aromatics measured at ground displayed a different pattern with two peaks occurring in the morning (LT 07:00–08:00) and evening (LT 19:00–22:00), respectively. Diurnal patterns of aromatics are consistent with that of NOx (a typical tracer of traffic emissions in urban region) at ground level but were different from that of NOx at 450 m (Figure 4). Therefore, measured concentrations of aromatics, particularly for benzene, were markedly affected by traffic emissions at ground level, but contributed by more complex sources at 450 m. The differences in diurnal profiles of aromatics between working and non-working days were insignificant (p>0.05), implying minor contributions from visitor-related emissions. On working days, toluene concentrations measured at 450 m were more affected by traffic emissions as manifested by the two remarkable peaks in the morning and late afternoon.

Isoprene and monoterpenes exhibited distinct diurnal variation patterns during the two campaigns. As reported in (Gómez et al., 2020; Tan et al., 2021), diurnal profiles of isoprene and monoterpenes concentrations in non-urban regions usually displayed unimodal patterns with a peak occurring at noon due to the strong light/temperature-dependence of biogenic emissions. In this study, isoprene concentrations at 450 m plateaued during the daytime and were slightly higher on non-working days than those on working days, implying large contributions from visitor-related emissions. The diurnal profile of monoterpenes measured at 450 m exhibited a bimodal pattern with two peaks at LT 14:00 and 20:00, which was roughly in accordance with diurnal peaks of visitor numbers on the 450-m platform. In addition, monoterpenes concentrations at 450 m were significantly (p<0.01) higher on non-working days (particularly during the busiest tourist hours) than on working days, confirming significant contributions from

303 visitor-related or cooking emissions (Klein et al., 2016). The diurnal profiles of methyl
304 vinyl ketone (MVK) + methacrolein (MACR) demonstrated similar shapes to ozone at
305 both 450 m and ground level with maxima occurring between LT 13:00–15:00 (Figure
306 4), consistent with MVK+MACR as photooxidation products of isoprene (Greenberg
307 et al., 1999; Zhao et al., 2021). The concentrations of MVK+MACR during the daytime
308 on non-working days were also significantly (p<0.01) higher than those on working
309 days, which are consistent with isoprene observations.
310 Acetone, methanol, and ethanol are abundant OVOC species in urban atmosphere.
311 Diurnal profiles of acetone measured at both 450 m and the ground level were
312 characterized by higher concentrations in the daytime, suggesting predominant
313 contributions from daytime sources, such as vegetation emissions and photooxidation
314 of hydrocarbons (Hu et al., 2013; Gkatzelis et al., 2021). In addition, acetone
315 concentrations at 450 m were higher on non-working days than on working days,
316 implying prominent contributions from visitor-related emissions. Diurnal profiles of
317 methanol and ethanol measured at ground level were characterized by a bimodal pattern
318 with two peaks occurring in the morning (LT 08:00) and evening (LT 20:00),
319 respectively, confirming strong contributions from traffic emissions. However,
320 methanol concentrations measured at 450 m exhibited weak diurnal variability and
321 lower concentrations on non-working days, indicating that they were less affected by
322 visitor-related emissions. The diurnal profile of ethanol at 450 m displayed two peaks
323 at LT 13:00 and 19:00, respectively, which was in accordance with the two busiest
324 tourist hours of the 450-m platform. In addition, ethanol concentrations at 450 m on
325 non-working days were significantly (p<0.01) higher than those on working days,
326 particularly in the opening hours of the 450-m platform. These results suggest that the
327 ethanol concentrations measured at 450 m were largely contributed by visitor-related
328 emissions.
329 To further explore spatial scales of emission source regions for different VOC
330 species, autocorrelation profiles of their time series were calculated by offsetting time

from -120 to 120 min. As indicated in previous studies (Hayes et al., 2013; Hu et al., 2016), concentrations of a species that is more affected by local sources would have a narrower autocorrelation profile. As shown in Figure 4, peak widths of autocorrelation profiles for different species at 450 m strongly varied. Autocorrelation profiles of monoterpenes, toluene, ethanol, methanol, and isoprene were relatively narrower (even narrower than the autocorrelation profile of NOx), and thus sources of these species had more local characteristics. Autocorrelation profiles of benzene, C8 aromatics, acetone, and MVK+MACR were much flatter (but narrower than the autocorrelation profile of ozone and Ox), indicating that concentrations of these species were more contributed by sources at larger spatial scales. By contrast, peak widths of the autocorrelation profiles for different species (except for ethanol) were comparable to that of NOx. Therefore, concentrations of the selected VOC species were notably contributed by local traffic emissions at ground level but contributed by more complex sources on larger spatial scales at 450 m.

3.3 Impacts of visitor-related emissions on VOCs measurements

As introduced in section 2.1, the CTT campaign was conducted in August-November of 2020, during which visitors were required to wear masks when visiting the CTT and ethanol-containing products were widely used to prevent the spread of the COVID-19 pandemic. For example, medicinal alcohol (75%) spray was widely used to wipe public utilities and 75%-ethanol bacteriostatic gel was extensively used as sanitizer for hands. The total usage of ethanol-containing products was closely associated with the number of visitors. This can be manifested by the diurnal profiles of some VOC species (e.g., ethanol) that exhibited similar variation patterns to that of the number of visitors at the 450-m platform, as shown in Figure 3. In addition, the restaurants are located ~30 m below the observation site and emission intensities of VOCs (e.g., monoterpenes) from cooking-related sources were also closely associated with the number of visitors. Therefore, the VOCs measurements were inevitably affected by visitor-related emissions, such as human breath, cooking, and volatilization

of ethanol-containing and personal care products (Veres et al., 2013).

As shown in Figure 5(a), the diurnal profile of CO_2 measured at 450 m increased between LT 09:00–20:00, which was different from those measured at ground level. The higher CO_2 mixing ratios at 450 m were predominantly contributed by human breath due to the absence of combustion sources. Measured ethanol mixing ratios were well correlated with those of CO_2 (R^2=0.36, p<0.01) during the CTT campaign (Figure 5(b)), indicating that ethanol concentrations, as well as its variations, were predominantly determined by the change in the number of visitors on the tower. In addition, the CO_2 mixing ratios on non-working days, especially during the busiest tourist hours, were significantly (p<0.01) higher than those on working days. The 450-m platform was closed during October 13-15 as the result of the influence of Typhoon Kompasu. On these days, mixing ratios of ethanol, CO_2, and monoterpenes exhibited similar variation patterns to benzene (a typical tracer of traffic emissions), as shown in Figure 5(c). However, mixing ratios of ethanol, CO_2, and monoterpenes exhibited quite different variation patterns from benzene when the 450-m platform was re-open (October 16–21). For instance, mixing ratios of ethanol, CO_2, and monoterpenes generally decreased from LT 12:00 to 18:00 between October 13–15, but markedly increased during the same period between October 16–21. Therefore, it can be concluded that the VOCs measurements made at 450 m were significantly affected by visitor-related emissions, which will be quantitatively assessed using the PMF analysis in following sections.

3.4 Source analysis of VOCs measurements

In this study, a five-factor solution for the PMF analysis was chosen as the optimal result. Figure 6 displays source profiles (m/z ≤ 150, the full range of the mass spectra is shown in Figure S7) of the five PMF factors along with average diurnal profiles of their contributions. The five factors were assigned to likely sources of daytime-mixed, visitor-related, vehicular+industrial, regional transport, and volatile chemical product (VCP)-dominated according to characteristics of their source profiles and temporal

387 variations, which are detailedly discussed in the *SI*.

388 The visitor-related source predominantly includes contributions from human
389 breath and volatilization of ethanol-containing and personal care products.
390 Contributions of the visitor-related source had the narrowest autocorrelation profile
391 among the five factors (Figure 6(g)), confirming its most local characteristics. As shown
392 in Figure 7, the visitor-related source had the largest contributions (15.9 ± 19.6 ppb),
393 accounting for 30% of the average TVOC mixing ratio. In addition, contributions of the
394 visitor-related source accounted for a larger fraction of TVOC mixing ratios on non-
395 working days (33%) than those on working days (28%), as shown in Figures 7 and S8.
396 The vehicular+industrial source mainly includes contributions from vehicular exhausts
397 and emissions of various industrial processes. Contributions of the vehicular+industrial
398 source (15.1 ± 18.3 ppb) were comparable to those of the visitor-related source,
399 accounting for 28% of the average TVOC mixing ratio. As anticipated, the
400 vehicular+industrial source contributed to a smaller fraction of TVOC mixing ratios on
401 non-working days (26%) than those on working days (30%). The VCP-dominated
402 source predominantly includes contributions from the volatilization of VCPs in urban
403 environments. The VCP-dominated source had an average contribution of 5.7 ± 5.4 ppb,
404 accounting for 11% of the average TVOC mixing ratio. The average contribution of the
405 VCP-dominated source in this study was comparable to those (~6.0 ppb) measured in
406 New York City (Gkatzelis et al., 2021). However, VCPs contributed to over 50% of
407 anthropogenic VOCs emissions in New York City, which is much greater than the
408 fraction in this study (11%, and it will increase to 16% when contributions of the visitor-
409 related source were removed). In comparison to large cities in U.S., traffic and
410 industrial emissions were still dominant sources of ambient VOCs in Chinese cities.
411 However, VCPs emissions should also be given more attention as the VCP-dominated
412 (22%) and vehicular+industrial (23%) sources had comparable contributions to the total
413 OH reactivities, as shown in Figure 7(f).

414 The daytime-mixed source predominantly includes contributions from biogenic

emissions and photooxidation products of various VOCs. The daytime-mixed source had an average contribution of 11.6 ± 12.6 ppb, accounting for 21% of the average TVOC mixing ratio. It exhibited consistent diurnal variation patterns on both working and non-working days but had larger contributions in the daytime on non-working days (Figure 6). This may be attributed to the enhanced formation of secondary OVOC species as manifested by the higher ozone concentrations on non-working days (Figure S9). The regional transport source mainly includes contributions from advection transport of aged air masses. Contributions of the regional transport source had the flattest autocorrelation profile, implying its most regional characteristics. Only a small fraction (<5%) of reactive chemical species such as aromatics were attributed to this factor, leading to the lowest contribution to the total OH reactivity. Contributions of the regional transport source accounted for 13% of the TVOC mixing ratio when affected by continental airflows, but only accounted for 3% when affected by marine airflows (Figure S10). By contrast, contributions of the other factors displayed weak dependences on wind direction.

As shown in Figure 8, source apportionment of the selected VOC species (Figure 3) discussed in section 3.2 were further investigated. The vehicular+industrial source had the largest contribution (36%) to benzene. The daytime-mixed source also contributed to 18% of measured benzene mixing ratios. In addition, more than 20% of benzene was attributed to the VCP-dominated source. In contrast to benzene, toluene was predominantly attributed to the vehicular+industrial (93%) and visitor-related (7%) sources. The average ratio of toluene to benzene was 5.7 ppb/ppb during the CTT campaign (Figure S11), further confirming primary contributions of toluene from vehicular and industrial emissions (Wu et al., 2016; Zhou et al., 2019; Xia et al., 2021). The vehicular+industrial source also accounted for the largest fractions of C8 and C9 aromatics. In addition, 26% of C8 aromatics and 38% of C9 aromatics were attributed to the VCP-dominated source. The other three sources in total contributed to less than 10% of concentrations of C8 and C9 aromatics. These results indicate that VCPs are

443 important sources of aromatics in urban environments but they were rarely identified
444 in previous studies.

445 Isoprene and monoterpenes are widely known tracers of biogenic emissions
446 (Millet et al., 2016; Zhao et al., 2021). However, the daytime-mixed source only
447 contributed to 16% of measured isoprene mixing ratios. By contrast, more than 70% of
448 isoprene were attributed to the visitor-related (38%) and VCP-dominated (35%) sources.
449 As for monoterpenes, more than 95% of the measured mixing ratios were attributed to
450 the visitor-related (47%) and VCP-dominated (49%) sources. The average ratio of
451 monoterpene to isoprene mixing ratios at 450 m was 0.84 in the daytime (LT 08:00–
452 18:00), which was significantly (p<0.01) greater than that at the ground level (0.05)
453 (Figure S11). It further confirms strong contributions of monoterpenes from visitor-
454 related emissions at the 450-m platform. The daytime-mixed source did not exhibit
455 discernible contributions to monoterpenes. This agrees well with the results in New
456 York City where monoterpene mixing ratios were primarily attributed to anthropogenic
457 sources such as VCPs, cooking, and building materials (Coggon et al., 2021; Gkatzelis
458 et al., 2021). These results suggest that emission intensities of isoprene and
459 monoterpenes may be highly underestimated in urban regions if their anthropogenic
460 emissions are overlooked or less considered. This is exceedingly important for air
461 quality models when estimating formation of ozone and secondary organic aerosol
462 driven by the oxidation of isoprene and monoterpene. As the key photooxidation
463 products of isoprene, nearly 60% of MVK+MACR were attributed to the daytime-
464 mixed source. The visitor-related, regional transport, and VCP-dominated sources
465 contributed to comparable fractions (11%–15%) of MVK+MACR. Therefore,
466 anthropogenic emissions are also important sources of MVK+MACR in urban
467 environments.

468 As shown in Figure 8, 39% of acetone was attributed to the daytime-mixed source.
469 The vehicular+industrial (19%) and VCP-dominated (21%) sources accounted for
470 comparable fractions of measured acetone mixing ratios. The visitor-related source had

471 the lowest contribution (7%) to acetone. As for methanol, the vehicular+industrial
472 source accounted for the largest fraction (38%), followed by the daytime-mixed (22%),
473 regional transport (17%), VCP-dominated (14%), and visitor-related (9%) sources.
474 These results reveal that VCPs also contributed significantly to ambient concentrations
475 of acetone and methanol and should be carefully considered when estimating their total
476 emission intensities from anthropogenic sources. Ethanol was predominantly attributed
477 to the visitor-related source. Therefore, the enhanced ethanol mixing ratios were not
478 capable of representing its characteristic concentrations in urban environments.
479 Although the absence of synchronous ground-level measurements, we can speculate
480 that ethanol concentrations at ground level were also increased during the outbreak of
481 the COVID-19 pandemic due to the extensive usage of ethanol-containing products.
482 The enhancement of ethanol concentrations can contribute significantly to the increase
483 in atmospheric OH reactivity (Millet et al., 2012; de Gouw et al., 2017; de Gouw et al.,
484 2018) and then regulate the formation of secondary pollutants. Therefore, impacts of
485 the ethanol enhancement on ambient air quality should be explicitly investigated in
486 future studies due to the wide report of ozone enhancement during the outbreak of the
487 COVID-19 pandemic (Huang et al., 2020; Qi et al., 2021).

488 Acetonitrile is widely used as a typical tracer of biomass burning sources in
489 previous studies (de Gouw et al., 2003b; Zhang et al., 2020; Tan et al., 2021). However,
490 biomass burning source was not identified in this study because acetonitrile was not
491 predominantly attributed to a single factor. In addition to the visitor-related source, the
492 other four sources also had large contributions to acetonitrile. As indicated by (Huangfu
493 et al., 2021), it is not always suitable, particularly in urban environments, to use absolute
494 concentrations of acetonitrile as the indication of biomass burning sources. The ratio of
495 acetonitrile to CO is a better indicator to identify whether VOCs measurements are
496 predominantly contributed by biomass burning emissions. The average ratio of
497 acetonitrile to CO was only 0.09 (ppb ppm^{-1}) during the CTT campaign (Figure S11),
498 indicating negligible contributions from biomass burning sources. In addition to the

daytime-mixed (22%) and vehicular+industrial (26%) sources, the VCP-dominated source (31%) also had large contributions to acetonitrile in urban environments.

3.5 Vertical distributions of air pollutants concentrations

As introduced in section 2.1, hourly concentrations of some air pollutants were routinely measured at four automatic sites on the CTT. Figure 9 shows contour plots of vertical profiles of NOx, ozone, Ox (O_3+NO_2), and $PM_{2.5}$ concentrations in September 2020. Concentrations of the four pollutants all exhibited stratified structures between 488 m and the ground level. Higher mixing ratios of ozone and Ox predominantly occurred at higher altitudes, while higher NOx mixing ratios mainly occurred at ground level. By contrast, higher $PM_{2.5}$ concentrations were observed at both middle altitudes and ground level.

To further clarify vertical distribution patterns of air pollutants concentrations, their composite profiles for daytime (LT 08:00–18:00), nighttime (LT 19:00–05:00), and the whole day in the campaign were determined, respectively, as shown in Figure 10. Vertical profiles of air pollutant concentrations exhibited similar shapes both in daytime and nighttime. NOx mixing ratios decreased from the ground level to 488 m, suggesting intensive surface emissions around the CTT. Ozone mixing ratios rapidly increased from the ground level to 488 m, which was consistent with the results reported in previous studies (Velasco et al., 2008; Li et al., 2018; Zhang et al., 2019; Li et al., 2021b). The positive gradients of ozone profiles are mainly caused by enhanced NO titration ($NO+O_3=O_2+NO_2$) and dry deposition near ground. Ox mixing ratios also increased from the ground level to 488 m but exhibited weaker gradients in comparison to ozone. Vertical profiles of $PM_{2.5}$ concentrations exhibited similar shapes to NOx. Daily mean concentrations of $PM_{2.5}$ and Ox were well correlated at the four altitudes with r values varying in the range of 0.61–0.82, suggesting prominent contributions of secondary formation to ambient PM concentrations. Moreover, the correlation coefficients between Ox and $PM_{2.5}$ concentrations at 488 m (0.82) were greater than those at ground level (0.78), as they were less affected by nearby vehicular emissions.

This is consistent with the work by (Yan et al., 2020), who reported that secondary components contributed to ~80% of $PM_{2.5}$ concentrations in PRD over the 2008–2019 period.

As shown in Figures 9 and 10, vertical profiles of air pollutant concentrations exhibited weaker gradients in the daytime than in the nighttime. Therefore, the daytime VOCs chemistry may have minor differences between the ground level and the 450-m site due to strong vertical mixing of chemical species in the planetary boundary layer (PBLH>450 m, as shown in Figure S12). In the nighttime, the oxidative products (such as organic nitrates and OVOCs) of unsaturated hydrocarbons, predominantly initiated by nitrate radicals (NO_3) and ozone, are also important precursors of secondary aerosol (Warneke et al., 2004; Brown et al., 2011; Ng et al., 2017; Liebmann et al., 2019). However, it is highly challenging to investigate the nighttime VOCs chemistry with only ground-level measurements due to the rapid removal of NO_3 radicals and ozone by enhanced NO titration (Geyer and Stutz, 2004; Stutz et al., 2004; Brown et al., 2007). In this condition, the nocturnal residual layer, separated from nocturnal boundary layer and remained, to a large extent, the chemical composition of the daytime atmosphere, could provide an ideal place for investigating nighttime VOCs chemistry. Oxidative products of VOCs in the residual layer could be mixed downward with the expansion of the PBL during the daytime (Geyer and Stutz, 2004; Stutz et al., 2004; Li et al., 2021a), contributing to the formation of ozone and secondary aerosol at ground level. Investigation of the nighttime VOCs chemistry was one of the initial purposes of this study. Unfortunately, the 450-m site was rarely located in the nocturnal residual layer during the CTT campaign due to frequent occurrences of cloudy and rainy weather. The average nighttime PBLH in Guangzhou was approximately stabilized at 500 m during the campaign (Figure S12), implying notable impacts from surface emissions on the measurements made at 450 m.

In addition to the measured PBLH data, formation of the residual layer at 450 m could be also identified by comparing differences of ozone mixing ratios between 488

m and the ground level. Without fresh NO emissions, ozone mixing ratios in the nocturnal residual layer were markedly higher than at ground level and exhibited weak variability throughout the nighttime (Caputi et al., 2019; Udina et al., 2020). By contrast, surface ozone mixing ratios are generally very low (close to zero) due to enhanced titration by freshly emitted NO and strong inhibition of atmospheric vertical mixing (Ma et al., 2011; Chen et al., 2020). In this study, the data collected between September 27–30 was one of the cases discussed above and was used to briefly describe behaviors of some representative VOC species (namely ethanol, monoterpene, styrene, phenol, and toluene) at 450 m.

As shown in Figure 11, ozone mixing ratios measured at ground level (10.2 ± 10.4 ppb) were significantly (p<0.01) lower than those at 488 m (44.2 ± 19.6 ppb) on the nighttime of September 27–30, indicating formation of the nocturnal residual layer lower than 450 m. On the nighttime of September 27–28, ozone mixing ratios at 488 m slightly fluctuated around 46.8 ppb between LT 19:00–00:00 and suddenly decreased to 28.4 ppb at LT 01:00 on September 28. The sudden decrease in ozone at LT 01:00 was accompanied by slight increases in both NOx and VOCs but notable decreases in NOx and NO at ground level, indicating a transitory intrusion of surface fresh emissions into the residual layer. On September 28, ozone mixing ratios at 488 m slightly decreased from 33.0 to 31.5 ppb from LT 02:00 to 05:00, during which mixing ratios of NOx and VOCs all decreased in different degrees. The continuous decreases in both toluene and ethanol between LT 02:00–05:00 confirm that the VOCs measurements at 450 m were free of interferences by fresh emissions due to their large contributions from vehicular exhausts (Figure 8). Toluene mixing ratios decreased by 43% from LT 02:00 to 05:00, which was larger than those (12–27%) of the other VOC species shown in Figure 11. However, the NO_3 reactivity (characterized by reaction rate constants of VOC species to NO_3 radical, k_{NO3}) of toluene (k_{NO3} = 7×10^{-17} cm^3 $molecule^{-1}$ s^{-1}) is exceedingly lower than those of the other unsaturated VOC species (k_{NO3} varies in the magnitudes of 10^{-12} cm^3 $molecule^{-1}$ s^{-1}) (Atkinson and Arey, 2003; Atkinson et al.,

583 2006). Therefore, the decline of unsaturated VOC species in the nocturnal residual layer
584 may not be all attributed to the degradation chemistry initiated by NO_3 radicals or ozone.
585 On the nighttime of September 28–29, the PBLH was higher than 500 m between
586 LT 19:00–00:00, resulting in notable decreases in ozone and increases in NOx and
587 VOCs. As shown in Figure 11, the 450-m site may locate in the residual layer after LT
588 01:00. However, the rapid decrease in mixing ratios of NOx and VOCs between LT
589 01:00–05:00 were not likely caused by chemical removal due to the rapid increase in
590 ozone. Regional transport of aged air masses (characterized by high ozone and low NOx
591 mixing ratios) may be responsible for the rapid decline in various VOC species in the
592 early morning of September 29. On the nighttime of September 29–30, the 450-m site
593 may be impacted by surface fresh emissions as mixing ratios of ozone, NOx, and VOCs
594 all decreased between LT 19:00–01:00 and simultaneously increased between LT
595 02:00–05:00. NOx and toluene mixing ratios generally increased between LT 12:00–
596 18:00 during September 27–29, which were quite different from their average diurnal
597 variation patterns during the whole campaign (Figures 3 and 4). As discussed above,
598 the 450-m site was located in the nocturnal residual layer during September 27–29.
599 Therefore, emissions of pollutants from surface sources could be mixed upward to the
600 measurement site only when the PBLH was higher than 450 m. Furthermore, the PBL
601 was relatively lower and rapidly shrank in the afternoon, leading to the accumulation
602 of chemical species at 450 m.
603 In summary, the VOCs measurements made by PTR-ToF-MS at the 450-m site
604 can be used to characterize variations in VOC species from their primary emissions
605 during the nighttime. Nevertheless, the oxidative degradation processes of VOCs in the
606 nighttime were not well captured. It is highly difficult to provide more information on
607 the nighttime chemistry of VOC species solely depending on their temporal variations.
608 We believe that the oxidative degradation of reactive VOC species did occur in the
609 nocturnal residual layer due to the coexistence of high concentrations of NOx and ozone.
610 Measurement techniques that targeting oxidation products (e.g., ToF-CIMS) and

numerical models should be jointly used to deeply analyze the nighttime chemistry of VOCs in the nocturnal residual layer and quantitatively evaluate their impacts on ambient air quality during the daytime.

4 Conclusions

Continuous measurements of VOCs mixing ratios were made by PTR-ToF-MS at 450 m on the CTT in PRD, China from August 18–November 5, 2020. In addition to some specific VOC species (such as ethanol and monoterpenes) that were intensively emitted by visitor-related sources, mixing ratios of most VOC species at 450 m were generally lower than those at ground level. Due to intensive emissions from visitor-related sources, mixing ratios of some VOC species were significantly higher on non-working days than those on working days. The VOCs mixing ratios measured at 450 m also exhibited different diurnal variations from those at ground level, indicating that they were contributed by more mixed sources at larger spatial scales. Five sources, namely daytime-mixed, visitor-related, vehicular+industrial, regional transport, and VCP-dominated, were determined by the PMF model, contributing to 21%, 30%, 28%, 10%, and 11% of the average TVOC mixing ratio, respectively. In addition to the daytime-mixed and visitor-related sources, the other three sources all had relatively lower contributions on non-working days than on working days. The VCP-dominated source contributed an average of 5.7 ppb to TVOC mixing ratios, which was comparable to those reported in American cities (Gkatzelis et al., 2021). However, the VCP-dominated source accounted for a much smaller fraction (11%) of measured TVOC mixing ratios in this study than in U.S. cities (>50%). Therefore, the reduction in anthropogenic VOC emissions from traffic and industrial sources are still priorities of current air pollution control for Chinese cities. Though smaller fraction of VOCs contributed by VCPs was observed in this study compared to cities in U.S. (McDonald et al., 2018; Gkatzelis et al., 2021), large fractions of key VOC species (such as monoterpenes and some aromatic species) were attributed to the VCP-dominated

source. In addition, the VCP-dominated (22%) and vehicular+industrial sources (23%) had comparable contributions to the total OH reactivity. Therefore, VCPs emissions should be given more attentions when making control strategies for VOCs in urban region..

The vertical distribution patterns of NOx, ozone, Ox, and $PM_{2.5}$ concentrations were investigated using measurements made at four different heights on the CTT. Vertical profiles of NOx and $PM_{2.5}$ generally exhibited negative gradients, while vertical profiles of ozone demonstrated positive gradients. In addition, the vertical gradients of air pollutant concentrations were larger in the nighttime than in the daytime, predominantly owing to stronger stability of the nocturnal boundary layer. The 450-m site was rarely located in the nocturnal residual layer as cloudy and rainy weather dominated during the campaign. The selected case revealed that the NO_3- or O_3-initiated degradation chemistry may be not the sole path for the removal of unsaturated VOC species in nighttime. The degradation chemistry of reactive VOC species in the nocturnal residual layer and their impacts on ground-level air quality could be further investigated in combination with model simulations in future studies.

Data availability

The observational data used in this study are available from corresponding authors upon request.

Author contributions

XBL and BY designed the research. XBL, BY, SHW, CLW, JL, ZJL, XJH, YBHF, CLP, CP, JPQ, CHW, YCY, MC, HDZ, WDY, XMW, and MS contributed to the data collection and data analysis. XBL and BY performed the PMF analysis with contributions from YXS, SXY, and SH. XBL and BY wrote the paper. All the coauthors discussed the results and reviewed the paper.

Competing interests

The authors declare that they have no conflict of interest.

Acknowledgments

This work was financially supported by the National Key R&D Plan of China (grant No. 2019YFE0106300), Guangdong Natural Science Funds for Distinguished Young Scholar (grant No. 2018B030306037), the National Natural Science Foundation of China (grant No. 41877302, 42121004), Key-Area Research and Development Program of Guangdong Province (grant No. 2020B1111360003), China Postdoctoral Science Foundation (grant No. 2019M663367), Guangdong Innovative and Entrepreneurial Research Team Program (grant No. 2016ZT06N263), and Special Fund Project for Science and Technology Innovation Strategy of Guangdong Province (grant No. 2019B121205004). We sincerely appreciate the help and support from the Canton Tower Management Team.

References

An, J., Huang, Y., Huang, C., Wang, X., Yan, R., Wang, Q., Wang, H., Jing, S., Zhang, Y., Liu, Y., Chen, Y., Xu, C., Qiao, L., Zhou, M., Zhu, S., Hu, Q., Lu, J., and Chen, C.: Emission inventory of air pollutants and chemical speciation for specific anthropogenic sources based on local measurements in the Yangtze River Delta region, China, Atmos. Chem. Phys., 21, 2003-2025, https://doi.org/10.5194/acp-21-2003-2021, 2021.

Atkinson, R., and Arey, J.: Atmospheric Degradation of Volatile Organic Compounds, Chem Rev, 103, 4605-4638, https://doi.org/10.1021/cr0206420, 2003.

Atkinson, R., Baulch, D. L., Cox, R. A., Crowley, J. N., Hampson, R. F., Hynes, R. G., Jenkin, M. E., Rossi, M. J., Troe, J., and Subcommittee, I.: Evaluated kinetic and photochemical data for atmospheric chemistry: Volume II – gas phase reactions of organic species, Atmos. Chem. Phys., 6, 3625-4055, https://doi.org/10.5194/acp-6-3625-2006, 2006.

Baudic, A., Gros, V., Sauvage, S., Locoge, N., Sanchez, O., Sarda-Estève, R., Kalogridis, C., Petit, J. E., Bonnaire, N., Baisnée, D., Favez, O., Albinet, A., Sciare, J., and Bonsang, B.: Seasonal variability and source apportionment of volatile organic compounds (VOCs) in the Paris megacity (France), Atmos. Chem. Phys., 16, 11961-11989, https://doi.org/10.5194/acp-16-11961-2016, 2016.

Benish, S. E., He, H., Ren, X., Roberts, S. J., Salawitch, R. J., Li, Z., Wang, F., Wang, Y., Zhang, F., Shao, M., Lu, S., and Dickerson, R. R.: Measurement report: Aircraft observations of ozone, nitrogen oxides, and volatile organic compounds over Hebei Province, China, Atmos. Chem. Phys., 20, 14523-14545, https://doi.org/10.5194/acp-20-14523-2020, 2020.

Brown, S. S., Dubé, W. P., Osthoff, H. D., Stutz, J., Ryerson, T. B., Wollny, A. G., Brock, C. A., Warneke, C., de Gouw, J. A., Atlas, E., Neuman, J. A., Holloway, J. S., Lerner, B. M., Williams, E. J., Kuster, W. C., Goldan, P. D., Angevine, W. M., Trainer, M., Fehsenfeld, F. C., and Ravishankara, A. R.: Vertical profiles in NO_3 and N_2O_5 measured from an aircraft: Results from the NOAA P-3 and surface platforms during the New England Air Quality Study 2004, Journal of Geophysical Research: Atmospheres, 112, https://doi.org/10.1029/2007JD008883, 2007.

Brown, S. S., Dubé, W. P., Peischl, J., Ryerson, T. B., Atlas, E., Warneke, C., de Gouw, J. A., te Lintel Hekkert, S., Brock, C. A., Flocke, F., Trainer, M., Parrish, D. D., Feshenfeld, F. C., and Ravishankara, A. R.: Budgets for nocturnal VOC oxidation by nitrate radicals aloft during the 2006 Texas Air Quality Study, Journal of Geophysical Research: Atmospheres, 116, https://doi.org/10.1029/2011JD016544, 2011.

Caputi, D. J., Faloona, I., Trousdell, J., Smoot, J., Falk, N., and Conley, S.: Residual layer ozone, mixing, and the nocturnal jet in California's San Joaquin Valley, Atmos. Chem. Phys., 19, 4721-4740, https://doi.org/10.5194/acp-19-4721-2019, 2019.

Chen, Q., Li, X.-B., Song, R., Wang, H.-W., Li, B., He, H.-D., and Peng, Z.-R.:

Development and utilization of hexacopter unmanned aerial vehicle platform to characterize vertical distribution of boundary layer ozone in wintertime, Atmospheric Pollution Research, 11, 1073-1083, https://doi.org/10.1016/j.apr.2020.04.002, 2020.

Chen, X., Millet, D. B., Singh, H. B., Wisthaler, A., Apel, E. C., Atlas, E. L., Blake, D. R., Bourgeois, I., Brown, S. S., Crounse, J. D., de Gouw, J. A., Flocke, F. M., Fried, A., Heikes, B. G., Hornbrook, R. S., Mikoviny, T., Min, K. E., Müller, M., Neuman, J. A., O'Sullivan, D. W., Peischl, J., Pfister, G. G., Richter, D., Roberts, J. M., Ryerson, T. B., Shertz, S. R., Thompson, C. R., Treadaway, V., Veres, P. R., Walega, J., Warneke, C., Washenfelder, R. A., Weibring, P., and Yuan, B.: On the sources and sinks of atmospheric VOCs: an integrated analysis of recent aircraft campaigns over North America, Atmos. Chem. Phys., 19, 9097-9123, https://doi.org/10.5194/acp-19-9097-2019, 2019.

Coggon, M. M., Gkatzelis, G. I., McDonald, B. C., Gilman, J. B., Schwantes, R. H., Abuhassan, N., Aikin, K. C., Arend, M. F., Berkoff, T. A., Brown, S. S., Campos, T. L., Dickerson, R. R., Gronoff, G., Hurley, J. F., Isaacman-VanWertz, G., Koss, A. R., Li, M., McKeen, S. A., Moshary, F., Peischl, J., Pospisilova, V., Ren, X., Wilson, A., Wu, Y., Trainer, M., and Warneke, C.: Volatile chemical product emissions enhance ozone and modulate urban chemistry, Proceedings of the National Academy of Sciences, 118, e2026653118, https://doi.org/10.1073/pnas.2026653118, 2021.

de Gouw, J., and Warneke, C.: Measurements of volatile organic compounds in the earth's atmosphere using proton-transfer-reaction mass spectrometry, Mass Spectrom Rev, 26, 223-257, https://doi.org/10.1002/mas.20119, 2007.

de Gouw, J. A., Goldan, P. D., Warneke, C., Kuster, W. C., Roberts, J. M., Marchewka, M., Bertman, S. B., Pszenny, A. A. P., and Keene, W. C.: Validation of proton transfer reaction-mass spectrometry (PTR-MS) measurements of gas-phase organic compounds in the atmosphere during the New England Air Quality Study (NEAQS) in 2002, Journal of Geophysical Research: Atmospheres, 108, https://doi.org/10.1029/2003jd003863, 2003a.

de Gouw, J. A., Warneke, C., Parrish, D. D., Holloway, J. S., Trainer, M., and Fehsenfeld, F. C.: Emission sources and ocean uptake of acetonitrile (CH3CN) in the atmosphere, Journal of Geophysical Research: Atmospheres, 108, https://doi.org/10.1029/2002JD002897, 2003b.

de Gouw, J. A., Gilman, J. B., Kim, S.-W., Lerner, B. M., Isaacman-VanWertz, G., McDonald, B. C., Warneke, C., Kuster, W. C., Lefer, B. L., Griffith, S. M., Dusanter, S., Stevens, P. S., and Stutz, J.: Chemistry of Volatile Organic Compounds in the Los Angeles basin: Nighttime Removal of Alkenes and Determination of Emission Ratios, Journal of Geophysical Research: Atmospheres, 122, 11,843-811,861, https://doi.org/10.1002/2017JD027459, 2017.

de Gouw, J. A., Gilman, J. B., Kim, S.-W., Alvarez, S. L., Dusanter, S., Graus, M., Griffith, S. M., Isaacman-VanWertz, G., Kuster, W. C., Lefer, B. L., Lerner, B. M., McDonald, B. C., Rappenglück, B., Roberts, J. M., Stevens, P. S., Stutz, J., Thalman, R., Veres, P. R., Volkamer, R., Warneke, C., Washenfelder, R. A., and Young, C. J.:

Chemistry of Volatile Organic Compounds in the Los Angeles Basin: Formation of Oxygenated Compounds and Determination of Emission Ratios, Journal of Geophysical Research: Atmospheres, 123, 2298-2319, https://doi.org/10.1002/2017JD027976, 2018.

Deming, B. L., Pagonis, D., Liu, X., Day, D. A., Talukdar, R., Krechmer, J. E., de Gouw, J. A., Jimenez, J. L., and Ziemann, P. J.: Measurements of delays of gas-phase compounds in a wide variety of tubing materials due to gas–wall interactions, Atmos. Meas. Tech., 12, 3453-3461, 10.5194/amt-12-3453-2019, 2019.

Dieu Hien, V. T., Lin, C., Thanh, V. C., Kim Oanh, N. T., Thanh, B. X., Weng, C.-E., Yuan, C.-S., and Rene, E. R.: An overview of the development of vertical sampling technologies for ambient volatile organic compounds (VOCs), J Environ Manage, 247, 401-412, https://doi.org/10.1016/j.jenvman.2019.06.090, 2019.

Fan, M.-Y., Zhang, Y.-L., Lin, Y.-C., Li, L., Xie, F., Hu, J., Mozaffar, A., and Cao, F.: Source apportionments of atmospheric volatile organic compounds in Nanjing, China during high ozone pollution season, Chemosphere, 263, 128025, https://doi.org/10.1016/j.chemosphere.2020.128025, 2021.

Fry, J. L., Brown, S. S., Middlebrook, A. M., Edwards, P. M., Campuzano-Jost, P., Day, D. A., Jimenez, J. L., Allen, H. M., Ryerson, T. B., Pollack, I., Graus, M., Warneke, C., de Gouw, J. A., Brock, C. A., Gilman, J., Lerner, B. M., Dubé, W. P., Liao, J., and Welti, A.: Secondary organic aerosol (SOA) yields from NO_3 radical + isoprene based on nighttime aircraft power plant plume transects, Atmos. Chem. Phys., 18, 11663-11682, https://doi.org/10.5194/acp-18-11663-2018, 2018.

Geng, F., Zhang, Q., Tie, X., Huang, M., Ma, X., Deng, Z., Yu, Q., Quan, J., and Zhao, C.: Aircraft measurements of O_3, NOx, CO, VOCs, and SO_2 in the Yangtze River Delta region, Atmos Environ, 43, 584-593, https://doi.org/10.1016/j.atmosenv.2008.10.021, 2009.

Geyer, A., and Stutz, J.: Vertical profiles of NO_3, N_2O_5, O_3, and NOx in the nocturnal boundary layer: 2. Model studies on the altitude dependence of composition and chemistry, Journal of Geophysical Research: Atmospheres, 109, https://doi.org/10.1029/2003jd004211, 2004.

Gkatzelis, G. I., Coggon, M. M., McDonald, B. C., Peischl, J., Gilman, J. B., Aikin, K. C., Robinson, M. A., Canonaco, F., Prevot, A. S. H., Trainer, M., and Warneke, C.: Observations Confirm that Volatile Chemical Products Are a Major Source of Petrochemical Emissions in U.S. Cities, Environ Sci Technol, https://doi.org/10.1021/acs.est.0c05471, 2021.

Gómez, M. C., Durana, N., García, J. A., de Blas, M., Sáez de Cámara, E., García-Ruiz, E., Gangoiti, G., Torre-Pascual, E., and Iza, J.: Long-term measurement of biogenic volatile organic compounds in a rural background area: Contribution to ozone formation, Atmos Environ, 224, 117315, https://doi.org/10.1016/j.atmosenv.2020.117315, 2020.

Greenberg, J. P., Guenther, A., Zimmerman, P., Baugh, W., Geron, C., Davis, K., Helmig, D., and Klinger, L. F.: Tethered balloon measurements of biogenic VOCs in

the atmospheric boundary layer, Atmos Environ, 33, 855-867, https://doi.org/10.1016/S1352-2310(98)00302-1, 1999.

Guo, H., Cheng, H. R., Ling, Z. H., Louie, P. K. K., and Ayoko, G. A.: Which emission sources are responsible for the volatile organic compounds in the atmosphere of Pearl River Delta?, J Hazard Mater, 188, 116-124, https://doi.org/10.1016/j.jhazmat.2011.01.081, 2011.

Hayes, P. L., Ortega, A. M., Cubison, M. J., Froyd, K. D., Zhao, Y., Cliff, S. S., Hu, W. W., Toohey, D. W., Flynn, J. H., Lefer, B. L., Grossberg, N., Alvarez, S., Rappenglück, B., Taylor, J. W., Allan, J. D., Holloway, J. S., Gilman, J. B., Kuster, W. C., de Gouw, J. A., Massoli, P., Zhang, X., Liu, J., Weber, R. J., Corrigan, A. L., Russell, L. M., Isaacman, G., Worton, D. R., Kreisberg, N. M., Goldstein, A. H., Thalman, R., Waxman, E. M., Volkamer, R., Lin, Y. H., Surratt, J. D., Kleindienst, T. E., Offenberg, J. H., Dusanter, S., Griffith, S., Stevens, P. S., Brioude, J., Angevine, W. M., and Jimenez, J. L.: Organic aerosol composition and sources in Pasadena, California, during the 2010 CalNex campaign, Journal of Geophysical Research: Atmospheres, 118, 9233-9257, https://doi.org/10.1002/jgrd.50530, 2013.

He, X., Yuan, B., Wu, C., Wang, S., Wang, C., Huangfu, Y., Qi, J., Ma, N., Xu, W., Wang, M., Chen, W., Su, H., Cheng, Y., and Shao, M.: Volatile organic compounds in wintertime North China Plain: Insights from measurements of proton transfer reaction time-of-flight mass spectrometer (PTR-ToF-MS), Journal of Environmental Sciences, https://doi.org/10.1016/j.jes.2021.08.010, 2022.

Hornbrook, R. S., Blake, D. R., Diskin, G. S., Fried, A., Fuelberg, H. E., Meinardi, S., Mikoviny, T., Richter, D., Sachse, G. W., Vay, S. A., Walega, J., Weibring, P., Weinheimer, A. J., Wiedinmyer, C., Wisthaler, A., Hills, A., Riemer, D. D., and Apel, E. C.: Observations of nonmethane organic compounds during ARCTAS − Part 1: Biomass burning emissions and plume enhancements, Atmos. Chem. Phys., 11, 11103-11130, 10.5194/acp-11-11103-2011, 2011.

Hu, L., Millet, D. B., Mohr, M. J., Wells, K. C., Griffis, T. J., and Helmig, D.: Sources and seasonality of atmospheric methanol based on tall tower measurements in the US Upper Midwest, Atmos. Chem. Phys., 11, 11145-11156, https://doi.org/10.5194/acp-11-11145-2011, 2011.

Hu, L., Millet, D. B., Kim, S. Y., Wells, K. C., Griffis, T. J., Fischer, E. V., Helmig, D., Hueber, J., and Curtis, A. J.: North American acetone sources determined from tall tower measurements and inverse modeling, Atmos. Chem. Phys., 13, 3379-3392, https://doi.org/10.5194/acp-13-3379-2013, 2013.

Hu, L., Millet, D. B., Baasandorj, M., Griffis, T. J., Travis, K. R., Tessum, C. W., Marshall, J. D., Reinhart, W. F., Mikoviny, T., Müller, M., Wisthaler, A., Graus, M., Warneke, C., and de Gouw, J.: Emissions of C6–C8 aromatic compounds in the United States: Constraints from tall tower and aircraft measurements, Journal of Geophysical Research: Atmospheres, 120, 826-842, https://doi.org/10.1002/2014JD022627, 2015a.

Hu, L., Millet, D. B., Baasandorj, M., Griffis, T. J., Turner, P., Helmig, D., Curtis, A. J., and Hueber, J.: Isoprene emissions and impacts over an ecological transition

region in the U.S. Upper Midwest inferred from tall tower measurements, Journal of Geophysical Research: Atmospheres, 120, 3553-3571, https://doi.org/10.1002/2014jd022732, 2015b.

Hu, W., Hu, M., Hu, W., Jimenez, J. L., Yuan, B., Chen, W., Wang, M., Wu, Y., Chen, C., Wang, Z., Peng, J., Zeng, L., and Shao, M.: Chemical composition, sources, and aging process of submicron aerosols in Beijing: Contrast between summer and winter, Journal of Geophysical Research: Atmospheres, 121, 1955-1977, https://doi.org/10.1002/2015JD024020, 2016.

Huang, X., Ding, A., Gao, J., Zheng, B., Zhou, D., Qi, X., Tang, R., Wang, J., Ren, C., Nie, W., Chi, X., Xu, Z., Chen, L., Li, Y., Che, F., Pang, N., Wang, H., Tong, D., Qin, W., Cheng, W., Liu, W., Fu, Q., Liu, B., Chai, F., Davis, S. J., Zhang, Q., and He, K.: Enhanced secondary pollution offset reduction of primary emissions during COVID-19 lockdown in China, National Science Review, 8, https://doi.org/10.1093/nsr/nwaa137, 2020.

Huangfu, Y., Yuan, B., Wang, S., Wu, C., He, X., Qi, J., de Gouw, J., Warneke, C., Gilman, J. B., Wisthaler, A., Karl, T., Graus, M., Jobson, B. T., and Shao, M.: Revisiting Acetonitrile as Tracer of Biomass Burning in Anthropogenic-Influenced Environments, Geophys Res Lett, 48, e2020GL092322, https://doi.org/10.1029/2020GL092322, 2021.

Jin, X., Li, Z., Wu, T., Wang, Y., Cheng, Y., Su, T., Wei, J., Ren, R., Wu, H., Li, S., Zhang, D., and Cribb, M.: The different sensitivities of aerosol optical properties to particle concentration, humidity, and hygroscopicity between the surface level and the upper boundary layer in Guangzhou, China, Sci Total Environ, 803, 150010, https://doi.org/10.1016/j.scitotenv.2021.150010, 2022.

Klein, F., Farren, N. J., Bozzetti, C., Daellenbach, K. R., Kilic, D., Kumar, N. K., Pieber, S. M., Slowik, J. G., Tuthill, R. N., Hamilton, J. F., Baltensperger, U., Prévôt, A. S. H., and El Haddad, I.: Indoor terpene emissions from cooking with herbs and pepper and their secondary organic aerosol production potential, Scientific Reports, 6, 36623, 10.1038/srep36623, 2016.

Koss, A., Yuan, B., Warneke, C., Gilman, J. B., Lerner, B. M., Veres, P. R., Peischl, J., Eilerman, S., Wild, R., Brown, S. S., Thompson, C. R., Ryerson, T., Hanisco, T., Wolfe, G. M., Clair, J. M. S., Thayer, M., Keutsch, F. N., Murphy, S., and de Gouw, J.: Observations of VOC emissions and photochemical products over US oil- and gas-producing regions using high-resolution H_3O^+ CIMS (PTR-ToF-MS), Atmospheric Measurement Techniques, 10, http://dx.doi.org/10.5194/amt-10-2941-2017, 2017.

Li, X.-B., Wang, D., Lu, Q.-C., Peng, Z.-R., Fu, Q., Hu, X.-M., Huo, J., Xiu, G., Li, B., Li, C., Wang, D.-S., and Wang, H.: Three-dimensional analysis of ozone and $PM_{2.5}$ distributions obtained by observations of tethered balloon and unmanned aerial vehicle in Shanghai, China, Stoch Env Res Risk A, 32, 1189-1203, https://doi.org/10.1007/s00477-018-1524-2, 2018.

Li, X.-B., Fan, G., Lou, S., Yuan, B., Wang, X., and Shao, M.: Transport and boundary layer interaction contribution to extremely high surface ozone levels in eastern China, Environ Pollut, 268, 115804,

https://doi.org/10.1016/j.envpol.2020.115804, 2021a.

Li, X.-B., Peng, Z.-R., Wang, D., Li, B., Huangfu, Y., Fan, G., Wang, H., and Lou, S.: Vertical distributions of boundary-layer ozone and fine aerosol particles during the emission control period of the G20 summit in Shanghai, China, Atmospheric Pollution Research, 12, 352-364, https://doi.org/10.1016/j.apr.2020.09.016, 2021b.

Li, X.-B., Yuan, B., Parrish, D. D., Chen, D., Song, Y., Yang, S., Liu, Z., and Shao, M.: Long-term trend of ozone in southern China reveals future mitigation strategy for air pollution, Atmos Environ, 269, 118869, 10.1016/j.atmosenv.2021.118869, 2022.

Liebmann, J., Sobanski, N., Schuladen, J., Karu, E., Hellén, H., Hakola, H., Zha, Q., Ehn, M., Riva, M., Heikkinen, L., Williams, J., Fischer, H., Lelieveld, J., and Crowley, J. N.: Alkyl nitrates in the boreal forest: formation via the NO_3^-, OH^- and O_3-induced oxidation of biogenic volatile organic compounds and ambient lifetimes, Atmos. Chem. Phys., 19, 10391-10403, https://doi.org/10.5194/acp-19-10391-2019, 2019.

Liu, B., Liang, D., Yang, J., Dai, Q., Bi, X., Feng, Y., Yuan, J., Xiao, Z., Zhang, Y., and Xu, H.: Characterization and source apportionment of volatile organic compounds based on 1-year of observational data in Tianjin, China, Environ Pollut, 218, 757-769, https://doi.org/10.1016/j.envpol.2016.07.072, 2016.

Liu, X., Deming, B., Pagonis, D., Day, D. A., Palm, B. B., Talukdar, R., Roberts, J. M., Veres, P. R., Krechmer, J. E., Thornton, J. A., de Gouw, J. A., Ziemann, P. J., and Jimenez, J. L.: Effects of gas–wall interactions on measurements of semivolatile compounds and small polar molecules, Atmos. Meas. Tech., 12, 3137-3149, 10.5194/amt-12-3137-2019, 2019.

Liu, Y., Wang, H., Jing, S., Zhou, M., Lou, S., Qu, K., Qiu, W., Wang, Q., Li, S., Gao, Y., Liu, Y., Li, X., Peng, Z.-R., Chen, J., and Lu, K.: Vertical Profiles of Volatile Organic Compounds in Suburban Shanghai, Adv Atmos Sci, 38, 1177-1187, https://doi.org/10.1007/s00376-021-0126-y, 2021.

Ma, Z., Zhang, X., Xu, J., Zhao, X., and Meng, W.: Characteristics of ozone vertical profile observed in the boundary layer around Beijing in autumn, Journal of Environmental Sciences, 23, 1316-1324, https://doi.org/10.1016/s1001-0742(10)60557-8, 2011.

McDonald, B. C., de Gouw, J. A., Gilman, J. B., Jathar, S. H., Akherati, A., Cappa, C. D., Jimenez, J. L., Lee-Taylor, J., Hayes, P. L., McKeen, S. A., Cui, Y. Y., Kim, S.-W., Gentner, D. R., Isaacman-VanWertz, G., Goldstein, A. H., Harley, R. A., Frost, G. J., Roberts, J. M., Ryerson, T. B., and Trainer, M.: Volatile chemical products emerging as largest petrochemical source of urban organic emissions, Science, 359, 760, https://doi.org/10.1126/science.aaq0524, 2018.

Millet, D. B., Apel, E., Henze, D. K., Hill, J., Marshall, J. D., Singh, H. B., and Tessum, C. W.: Natural and Anthropogenic Ethanol Sources in North America and Potential Atmospheric Impacts of Ethanol Fuel Use, Environ Sci Technol, 46, 8484-8492, https://doi.org/10.1021/es300162u, 2012.

Millet, D. B., Baasandorj, M., Hu, L., Mitroo, D., Turner, J., and Williams, B. J.:

Nighttime Chemistry and Morning Isoprene Can Drive Urban Ozone Downwind of a Major Deciduous Forest, Environ Sci Technol, 50, 4335-4342, https://doi.org/10.1021/acs.est.5b06367, 2016.

Mo, Z., Shao, M., and Lu, S.: Compilation of a source profile database for hydrocarbon and OVOC emissions in China, Atmos Environ, 143, 209-217, https://doi.org/10.1016/j.atmosenv.2016.08.025, 2016.

Mo, Z., Huang, S., Yuan, B., Pei, C., Song, Q., Qi, J., Wang, M., Wang, B., Wang, C., Li, M., Zhang, Q., and Shao, M.: Deriving emission fluxes of volatile organic compounds from tower observation in the Pearl River Delta, China, Sci Total Environ, 741, 139763, https://doi.org/10.1016/j.scitotenv.2020.139763, 2020.

Müller, M., Anderson, B. E., Beyersdorf, A. J., Crawford, J. H., Diskin, G. S., Eichler, P., Fried, A., Keutsch, F. N., Mikoviny, T., Thornhill, K. L., Walega, J. G., Weinheimer, A. J., Yang, M., Yokelson, R. J., and Wisthaler, A.: In situ measurements and modeling of reactive trace gases in a small biomass burning plume, Atmos. Chem. Phys., 16, 3813-3824, 10.5194/acp-16-3813-2016, 2016.

Ng, N. L., Brown, S. S., Archibald, A. T., Atlas, E., Cohen, R. C., Crowley, J. N., Day, D. A., Donahue, N. M., Fry, J. L., Fuchs, H., Griffin, R. J., Guzman, M. I., Herrmann, H., Hodzic, A., Iinuma, Y., Jimenez, J. L., Kiendler-Scharr, A., Lee, B. H., Luecken, D. J., Mao, J. Q., McLaren, R., Mutzel, A., Osthoff, H. D., Ouyang, B., Picquet-Varrault, B., Platt, U., Pye, H. O. T., Rudich, Y., Schwantes, R. H., Shiraiwa, M., Stutz, J., Thornton, J. A., Tilgner, A., Williams, B. J., and Zaveri, R. A.: Nitrate radicals and biogenic volatile organic compounds: oxidation, mechanisms, and organic aerosol, Atmos. Chem. Phys., 17, 2103-2162, https://doi.org/10.5194/acp-17-2103-2017, 2017.

Pallavi, Sinha, B., and Sinha, V.: Source apportionment of volatile organic compounds in the northwest Indo-Gangetic Plain using a positive matrix factorization model, Atmos. Chem. Phys., 19, 15467-15482, https://doi.org/10.5194/acp-19-15467-2019, 2019.

Pernov, J. B., Bossi, R., Lebourgeois, T., Nøjgaard, J. K., Holzinger, R., Hjorth, J. L., and Skov, H.: Atmospheric VOC measurements at a High Arctic site: characteristics and source apportionment, Atmos. Chem. Phys., 21, 2895-2916, https://doi.org/10.5194/acp-21-2895-2021, 2021.

Qi, J., Mo, Z., Yuan, B., Huang, S., Huangfu, Y., Wang, Z., Li, X., Yang, S., Wang, W., Zhao, Y., Wang, X., Wang, W., Liu, K., and Shao, M.: An observation approach in evaluation of ozone production to precursor changes during the COVID-19 lockdown, Atmos Environ, 262, 118618, https://doi.org/10.1016/j.atmosenv.2021.118618, 2021.

Qin, J., Wang, X., Yang, Y., Qin, Y., Shi, S., Xu, P., Chen, R., Zhou, X., Tan, J., and Wang, X.: Source apportionment of VOCs in a typical medium-sized city in North China Plain and implications on control policy, Journal of Environmental Sciences, 107, 26-37, https://doi.org/10.1016/j.jes.2020.10.005, 2021.

Sangiorgi, G., Ferrero, L., Perrone, M. G., Bolzacchini, E., Duane, M., and Larsen, B. R.: Vertical distribution of hydrocarbons in the low troposphere below and above the

mixing height: Tethered balloon measurements in Milan, Italy, Environ Pollut, 159, 3545-3552, https://doi.org/10.1016/j.envpol.2011.08.012, 2011.

Squires, F. A., Nemitz, E., Langford, B., Wild, O., Drysdale, W. S., Acton, W. J. F., Fu, P., Grimmond, C. S. B., Hamilton, J. F., Hewitt, C. N., Hollaway, M., Kotthaus, S., Lee, J., Metzger, S., Pingintha-Durden, N., Shaw, M., Vaughan, A. R., Wang, X., Wu, R., Zhang, Q., and Zhang, Y.: Measurements of traffic-dominated pollutant emissions in a Chinese megacity, Atmos. Chem. Phys., 20, 8737-8761, https://doi.org/10.5194/acp-20-8737-2020, 2020.

Stutz, J., Alicke, B., Ackermann, R., Geyer, A., White, A., and Williams, E.: Vertical profiles of NO_3, N_2O_5, O_3, and NO_x in the nocturnal boundary layer: 1. Observations during the Texas Air Quality Study 2000, Journal of Geophysical Research: Atmospheres, 109, https://doi.org/10.1029/2003jd004209, 2004.

Tan, Y., Han, S., Chen, Y., Zhang, Z., Li, H., Li, W., Yuan, Q., Li, X., Wang, T., and Lee, S.-c.: Characteristics and source apportionment of volatile organic compounds (VOCs) at a coastal site in Hong Kong, Sci Total Environ, 777, 146241, https://doi.org/10.1016/j.scitotenv.2021.146241, 2021.

Ting, M., Yue-si, W., Jie, J., Fang-kun, W., and Mingxing, W.: The vertical distributions of VOCs in the atmosphere of Beijing in autumn, Sci Total Environ, 390, 97-108, https://doi.org/10.1016/j.scitotenv.2007.08.035, 2008.

Udina, M., Soler, M. R., Olid, M., Jiménez-Esteve, B., and Bech, J.: Pollutant vertical mixing in the nocturnal boundary layer enhanced by density currents and low-level jets: two representative case studies, Bound-lay Meteorol, 174, 203-230, https://doi.org/10.1007/s10546-019-00483-y, 2020.

Ulbrich, I. M., Canagaratna, M. R., Zhang, Q., Worsnop, D. R., and Jimenez, J. L.: Interpretation of organic components from Positive Matrix Factorization of aerosol mass spectrometric data, Atmos. Chem. Phys., 9, 2891-2918, https://doi.org/10.5194/acp-9-2891-2009, 2009.

Velasco, E., Marquez, C., Bueno, E., Bernabe, R. M., Sanchez, A., Fentanes, O., Wohrnschimmel, H., Cardenas, B., Kamilla, A., Wakamatsu, S., and Molina, L. T.: Vertical distribution of ozone and VOCs in the low boundary layer of Mexico City, Atmos. Chem. Phys., 8, 3061-3079, https://doi.org/10.5194/acp-8-3061-2008, 2008.

Veres, P. R., Faber, P., Drewnick, F., Lelieveld, J., and Williams, J.: Anthropogenic sources of VOC in a football stadium: Assessing human emissions in the atmosphere, Atmos Environ, 77, 1052-1059, https://doi.org/10.1016/j.atmosenv.2013.05.076, 2013.

Vo, T.-D.-H., Lin, C., Weng, C.-E., Yuan, C.-S., Lee, C.-W., Hung, C.-H., Bui, X.-T., Lo, K.-C., and Lin, J.-X.: Vertical stratification of volatile organic compounds and their photochemical product formation potential in an industrial urban area, J Environ Manage, 217, 327-336, https://doi.org/10.1016/j.jenvman.2018.03.101, 2018.

Wang, C., Yuan, B., Wu, C., Wang, S., Qi, J., Wang, B., Wang, Z., Hu, W., Chen, W., Ye, C., Wang, W., Sun, Y., Wang, C., Huang, S., Song, W., Wang, X., Yang, S., Zhang, S., Xu, W., Ma, N., Zhang, Z., Jiang, B., Su, H., Cheng, Y., Wang, X., and Shao, M.: Measurements of higher alkanes using NO+ chemical ionization in PTR-ToF-MS:

1010 important contributions of higher alkanes to secondary organic aerosols in China,
1011 Atmos. Chem. Phys., 20, 14123-14138, https://doi.org/10.5194/acp-20-14123-2020,
1012 2020a.
1013 Wang, T., Xue, L., Brimblecombe, P., Lam, Y. F., Li, L., and Zhang, L.: Ozone
1014 pollution in China: A review of concentrations, meteorological influences, chemical
1015 precursors, and effects, Sci Total Environ, 575, 1582-1596,
1016 https://doi.org/10.1016/j.scitotenv.2016.10.081, 2017.
1017 Wang, Y., Wang, Y., Tang, G., Yang, Y., Li, X., Yao, D., Wu, S., Kang, Y., Wang,
1018 M., and Wang, Y.: High gaseous carbonyl concentrations in the upper boundary layer
1019 in Shijiazhuang, China, Sci Total Environ, 799, 149438,
1020 https://doi.org/10.1016/j.scitotenv.2021.149438, 2021.
1021 Wang, Y. H., Gao, W. K., Wang, S., Song, T., Gong, Z. Y., Ji, D. S., Wang, L. L.,
1022 Liu, Z. R., Tang, G. Q., Huo, Y. F., Tian, S. L., Li, J. Y., Li, M. G., Yang, Y., Chu, B. W.,
1023 Petaja, T., Kerminen, V. M., He, H., Hao, J. M., Kulmala, M., Wang, Y. S., and Zhang,
1024 Y. H.: Contrasting trends of $PM_{2.5}$ and surface-ozone concentrations in China from 2013
1025 to 2017, National Science Review, 7, 1331-1339, https://doi.org/10.1093/nsr/nwaa032,
1026 2020b.
1027 Wang, Z., Yuan, B., Ye, C., Roberts, J., Wisthaler, A., Lin, Y., Li, T., Wu, C., Peng,
1028 Y., Wang, C., Wang, S., Yang, S., Wang, B., Qi, J., Wang, C., Song, W., Hu, W., Wang,
1029 X., Xu, W., Ma, N., Kuang, Y., Tao, J., Zhang, Z., Su, H., Cheng, Y., Wang, X., and
1030 Shao, M.: High Concentrations of Atmospheric Isocyanic Acid (HNCO) Produced from
1031 Secondary Sources in China, Environ Sci Technol, 54, 11818-11826,
1032 https://doi.org/10.1021/acs.est.0c02843, 2020c.
1033 Warneke, C., de Gouw, J. A., Goldan, P. D., Kuster, W. C., Williams, E. J., Lerner,
1034 B. M., Jakoubek, R., Brown, S. S., Stark, H., Aldener, M., Ravishankara, A. R., Roberts,
1035 J. M., Marchewka, M., Bertman, S., Sueper, D. T., McKeen, S. A., Meagher, J. F., and
1036 Fehsenfeld, F. C.: Comparison of daytime and nighttime oxidation of biogenic and
1037 anthropogenic VOCs along the New England coast in summer during New England Air
1038 Quality Study 2002, Journal of Geophysical Research: Atmospheres, 109,
1039 https://doi.org/10.1029/2003jd004424, 2004.
1040 Wu, C., Wang, C., Wang, S., Wang, W., Yuan, B., Qi, J., Wang, B., Wang, H., Wang,
1041 C., Song, W., Wang, X., Hu, W., Lou, S., Ye, C., Peng, Y., Wang, Z., Huangfu, Y., Xie,
1042 Y., Zhu, M., Zheng, J., Wang, X., Jiang, B., Zhang, Z., and Shao, M.: Measurement
1043 report: Important contributions of oxygenated compounds to emissions and chemistry
1044 of volatile organic compounds in urban air, Atmos. Chem. Phys., 20, 14769-14785,
1045 https://doi.org/10.5194/acp-20-14769-2020, 2020a.
1046 Wu, F., Yu, Y., Sun, J., Zhang, J., Wang, J., Tang, G., and Wang, Y.: Characteristics,
1047 source apportionment and reactivity of ambient volatile organic compounds at Dinghu
1048 Mountain in Guangdong Province, China, Sci Total Environ, 548-549, 347-359,
1049 https://doi.org/10.1016/j.scitotenv.2015.11.069, 2016.
1050 Wu, S., Tang, G., Wang, Y., Yang, Y., Yao, D., Zhao, W., Gao, W., Sun, J., and
1051 Wang, Y.: Vertically decreased VOC concentration and reactivity in the planetary

boundary layer in winter over the North China Plain, Atmos Res, 240, 104930, https://doi.org/10.1016/j.atmosres.2020.104930, 2020b.

Wu, S., Tang, G. Q., Wang, Y. H., Mai, R., Yao, D., Kang, Y. Y., Wang, Q. L., and Wang, Y. S.: Vertical Evolution of Boundary Layer Volatile Organic Compounds in Summer over the North China Plain and the Differences with Winter, Adv Atmos Sci, 38, 1165-1176, https://doi.org/10.1007/s00376-020-0254-9, 2021.

Xia, S.-Y., Wang, C., Zhu, B., Chen, X., Feng, N., Yu, G.-H., and Huang, X.-F.: Long-term observations of oxygenated volatile organic compounds (OVOCs) in an urban atmosphere in southern China, 2014–2019, Environ Pollut, 270, 116301, https://doi.org/10.1016/j.envpol.2020.116301, 2021.

Xue, L., Wang, T., Simpson, I. J., Ding, A., Gao, J., Blake, D. R., Wang, X., Wang, W., Lei, H., and Jin, D.: Vertical distributions of non-methane hydrocarbons and halocarbons in the lower troposphere over northeast China, Atmos Environ, 45, 6501-6509, https://doi.org/10.1016/j.atmosenv.2011.08.072, 2011.

Yan, F., Chen, W., Jia, S., Zhong, B., Yang, L., Mao, J., Chang, M., Shao, M., Yuan, B., Situ, S., Wang, X., Chen, D., and Wang, X.: Stabilization for the secondary species contribution to $PM_{2.5}$ in the Pearl River Delta (PRD) over the past decade, China: A meta-analysis, Atmos Environ, 242, 117817, https://doi.org/10.1016/j.atmosenv.2020.117817, 2020.

Ye, C., Yuan, B., Lin, Y., Wang, Z., Hu, W., Li, T., Chen, W., Wu, C., Wang, C., Huang, S., Qi, J., Wang, B., Wang, C., Song, W., Wang, X., Zheng, E., Krechmer, J. E., Ye, P., Zhang, Z., Wang, X., Worsnop, D. R., and Shao, M.: Chemical characterization of oxygenated organic compounds in the gas phase and particle phase using iodide CIMS with FIGAERO in urban air, Atmos. Chem. Phys., 21, 8455-8478, https://doi.org/10.5194/acp-21-8455-2021, 2021.

Yuan, B., Shao, M., de Gouw, J., Parrish, D. D., Lu, S., Wang, M., Zeng, L., Zhang, Q., Song, Y., Zhang, J., and Hu, M.: Volatile organic compounds (VOCs) in urban air: How chemistry affects the interpretation of positive matrix factorization (PMF) analysis, Journal of Geophysical Research: Atmospheres, 117, https://doi.org/10.1029/2012jd018236, 2012.

Yuan, B., Koss, A., Warneke, C., Gilman, J. B., Lerner, B. M., Stark, H., and de Gouw, J. A.: A high-resolution time-of-flight chemical ionization mass spectrometer utilizing hydronium ions (H_3O^+ ToF-CIMS) for measurements of volatile organic compounds in the atmosphere, Atmospheric Measurement Techniques, 9, 2735-2752, https://doi.org/10.5194/amt-9-2735-2016, 2016.

Yuan, B., Koss, A. R., Warneke, C., Coggon, M., Sekimoto, K., and de Gouw, J. A.: Proton-Transfer-Reaction Mass Spectrometry: Applications in Atmospheric Sciences, Chem Rev, 117, 13187-13229, https://doi.org/10.1021/acs.chemrev.7b00325, 2017.

Yuan, Z., Zhong, L., Lau, A. K. H., Yu, J. Z., and Louie, P. K. K.: Volatile organic compounds in the Pearl River Delta: Identification of source regions and recommendations for emission-oriented monitoring strategies, Atmos Environ, 76, 162-

172, https://doi.org/10.1016/j.atmosenv.2012.11.034, 2013.

Zhang, H., Zhang, Y., Huang, Z., Acton, W. J. F., Wang, Z., Nemitz, E., Langford, B., Mullinger, N., Davison, B., Shi, Z., Liu, D., Song, W., Yang, W., Zeng, J., Wu, Z., Fu, P., Zhang, Q., and Wang, X.: Vertical profiles of biogenic volatile organic compounds as observed online at a tower in Beijing, J Environ Sci (China), 95, 33-42, https://doi.org/10.1016/j.jes.2020.03.032, 2020.

Zhang, K., Xiu, G., Zhou, L., Bian, Q., Duan, Y., Fei, D., Wang, D., and Fu, Q.: Vertical distribution of volatile organic compounds within the lower troposphere in late spring of Shanghai, Atmos Environ, 186, 150-157, https://doi.org/10.1016/j.atmosenv.2018.03.044, 2018.

Zhang, K., Zhou, L., Fu, Q., Yan, L., Bian, Q., Wang, D., and Xiu, G.: Vertical distribution of ozone over Shanghai during late spring: A balloon-borne observation, Atmos Environ, 208, 48-60, https://doi.org/10.1016/j.atmosenv.2019.03.011, 2019.

Zhang, Y., Wang, X., Barletta, B., Simpson, I. J., Blake, D. R., Fu, X., Zhang, Z., He, Q., Liu, T., Zhao, X., and Ding, X.: Source attributions of hazardous aromatic hydrocarbons in urban, suburban and rural areas in the Pearl River Delta (PRD) region, J Hazard Mater, 250-251, 403-411, https://doi.org/10.1016/j.jhazmat.2013.02.023, 2013.

Zhao, D., Pullinen, I., Fuchs, H., Schrade, S., Wu, R., Acir, I. H., Tillmann, R., Rohrer, F., Wildt, J., Guo, Y., Kiendler-Scharr, A., Wahner, A., Kang, S., Vereecken, L., and Mentel, T. F.: Highly oxygenated organic molecule (HOM) formation in the isoprene oxidation by NO_3 radical, Atmos. Chem. Phys., 21, 9681-9704, https://doi.org/10.5194/acp-21-9681-2021, 2021.

Zheng, J., Yu, Y., Mo, Z., Zhang, Z., Wang, X., Yin, S., Peng, K., Yang, Y., Feng, X., and Cai, H.: Industrial sector-based volatile organic compound (VOC) source profiles measured in manufacturing facilities in the Pearl River Delta, China, Sci Total Environ, 456-457, 127-136, https://doi.org/10.1016/j.scitotenv.2013.03.055, 2013.

Zhou, X., Li, Z., Zhang, T., Wang, F., Wang, F., Tao, Y., Zhang, X., Wang, F., and Huang, J.: Volatile organic compounds in a typical petrochemical industrialized valley city of northwest China based on high-resolution PTR-MS measurements: Characterization, sources and chemical effects, Sci Total Environ, 671, 883-896, https://doi.org/10.1016/j.scitotenv.2019.03.283, 2019.

Zhu, B., Han, Y., Wang, C., Huang, X., Xia, S., Niu, Y., Yin, Z., and He, L.: Understanding primary and secondary sources of ambient oxygenated volatile organic compounds in Shenzhen utilizing photochemical age-based parameterization method, Journal of Environmental Sciences, 75, 105-114, https://doi.org/10.1016/j.jes.2018.03.008, 2019.

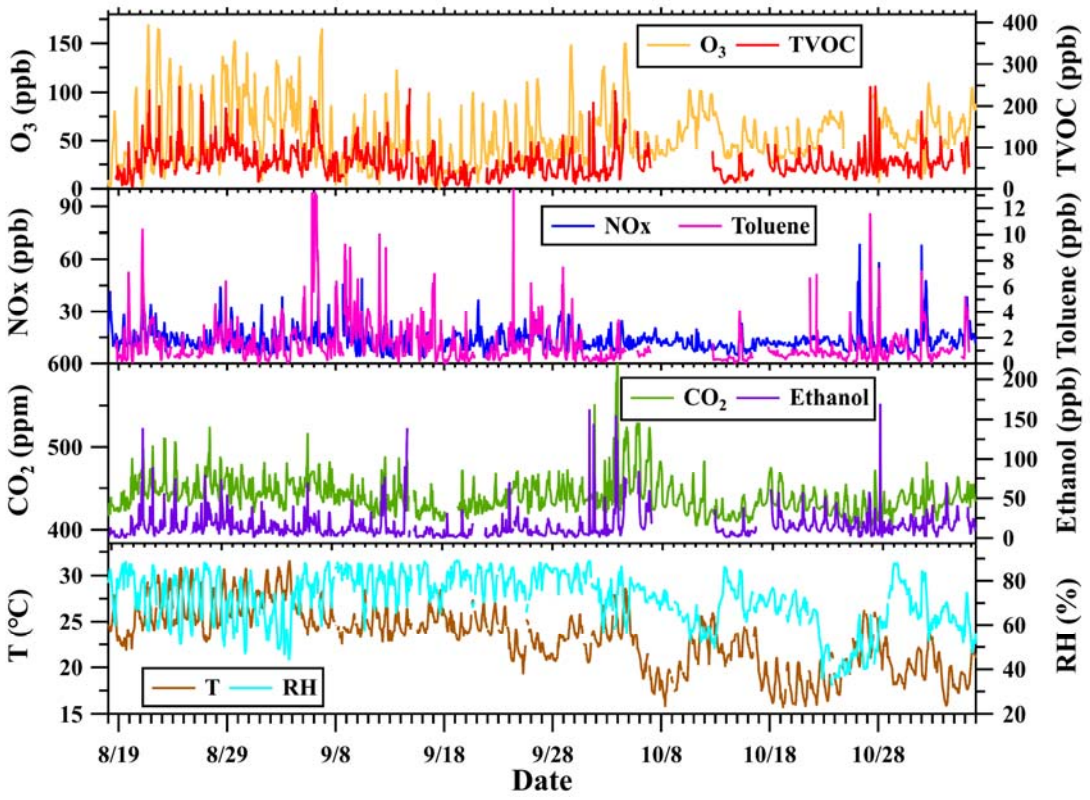

Figure 1. Time series of concentrations of some typical chemical species along with meteorological parameters (hourly averages) during the CTT campaign. Temperature (T), relative humidity (RH), concentrations of ozone and NOx were measured at 488 m. Concentrations of VOCs, ethanol, and CO_2 were measured at 450 m.

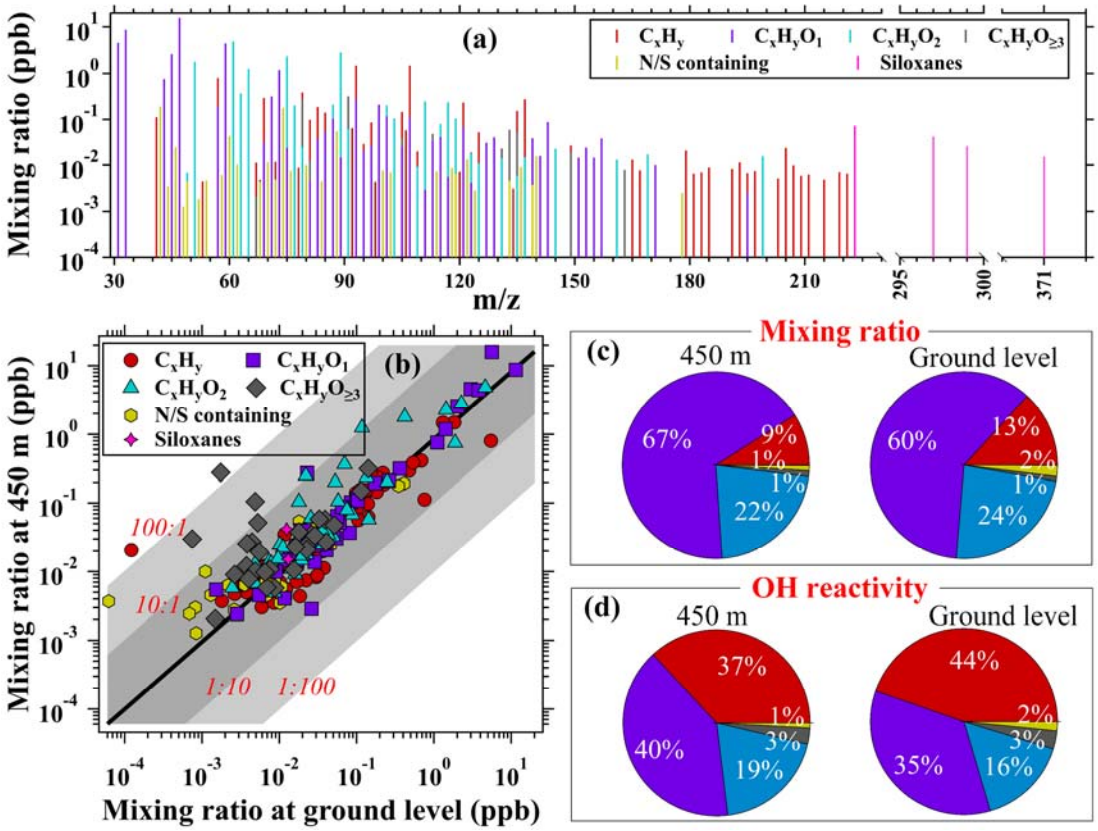

Figure 2. (a) Average mass spectra of VOCs (including 225 species) obtained by PTR-ToF-MS measured at 450 m during the CTT campaign. (b) Scatter plots of the average VOC mixing ratios measured at 450 m during the CTT campaign versus those measured at ground level during the GIG campaign; The black solid line indicates the ratio of 1:1; The dark grey shaded areas indicate the ratios of 10:1 and 1:10; The light grey shaded areas indicate the ratios of 100:1 and 1:100. (c-d) Average contribution percentages of the six VOCs categories to their total concentrations and OH reactivities at 450 m and the ground level, respectively; Only the VOCs species that have known reaction rate constants with OH radical (Table S1) were used for calculation.

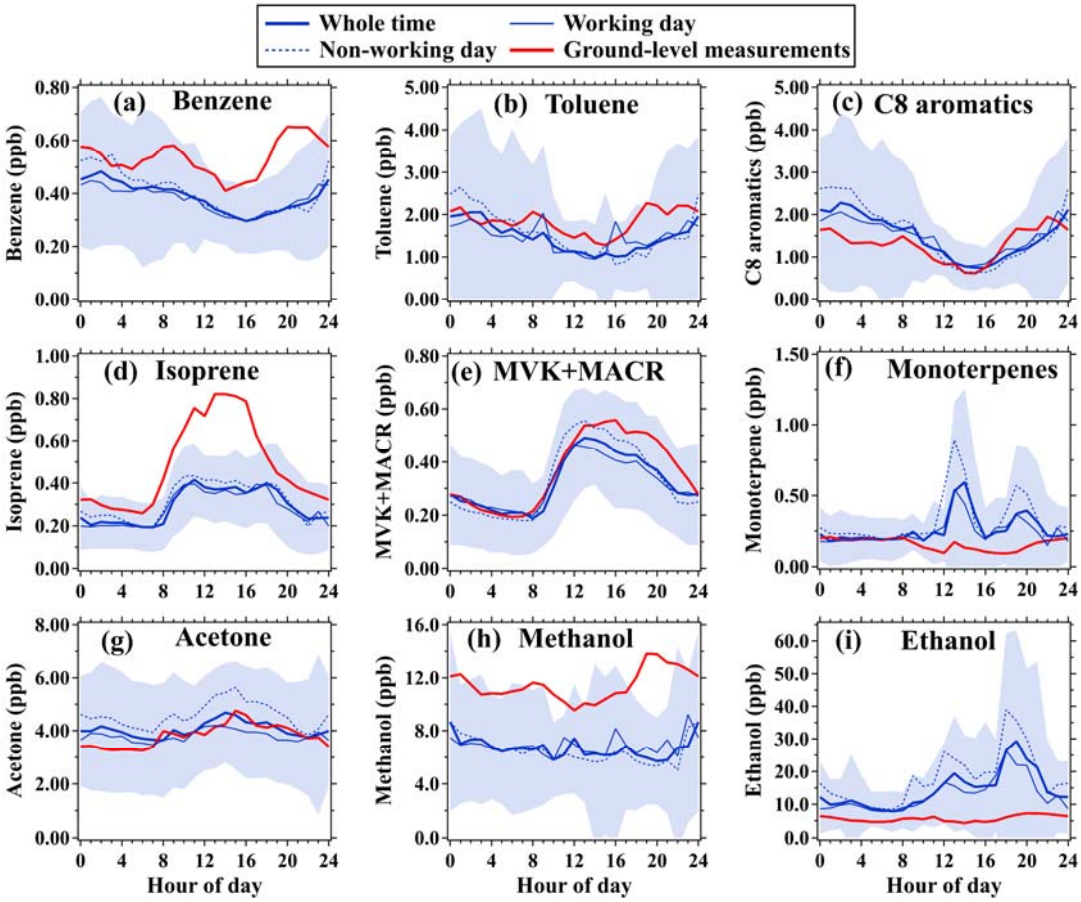

Figure 3. Diurnal variations in mixing ratios of selected VOC species measured by PTR-ToF-MS. Thick blue solid lines and shaded areas represent averages and standard deviations, respectively, during the CTT campaign (August 18–November 05, 2020). Red solid lines represent averages during the GIG campaign (September 11–November 19, 2018). Thin blue solid and dashed lines represent averages in working days and non-working (including weekends and public holidays) days, respectively, during the CTT campaign.

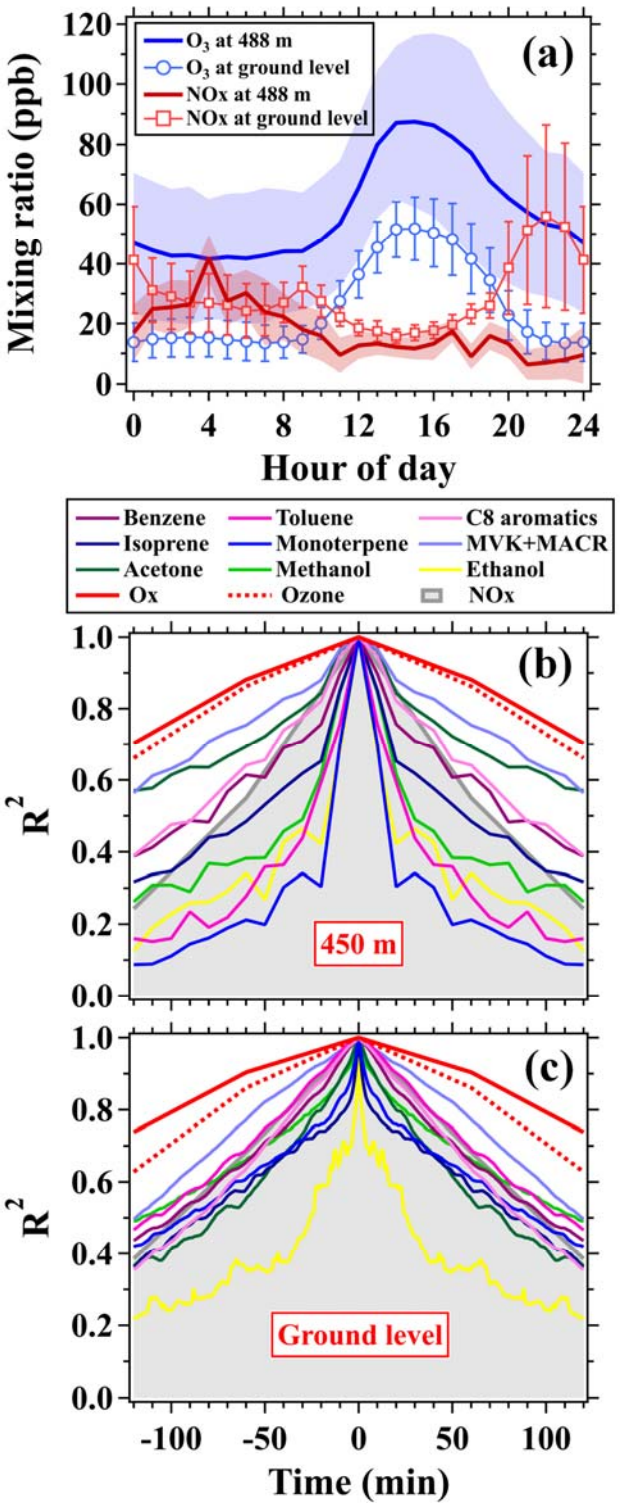

Figure 4. (a) Diurnal profiles of ozone and NOx mixing ratios measured at the 488-m site (mean ± standard deviation) and the surface site (mean ± 0.5 standard deviation) on the CTT. (b) Autocorrelation of the time series of ozone (488 m), NOx (488 m), Ox (488 m), and selected VOC species (450 m) during the CTT campaign. (c) Autocorrelation of the time series of the selected VOC species at ground level during

the GIG campaign; Autocorrelation of the time series of ozone, NOx, and Ox in panel (c) are calculated using the measurements made at the surface site of Canton Tower during the CTT campaign.

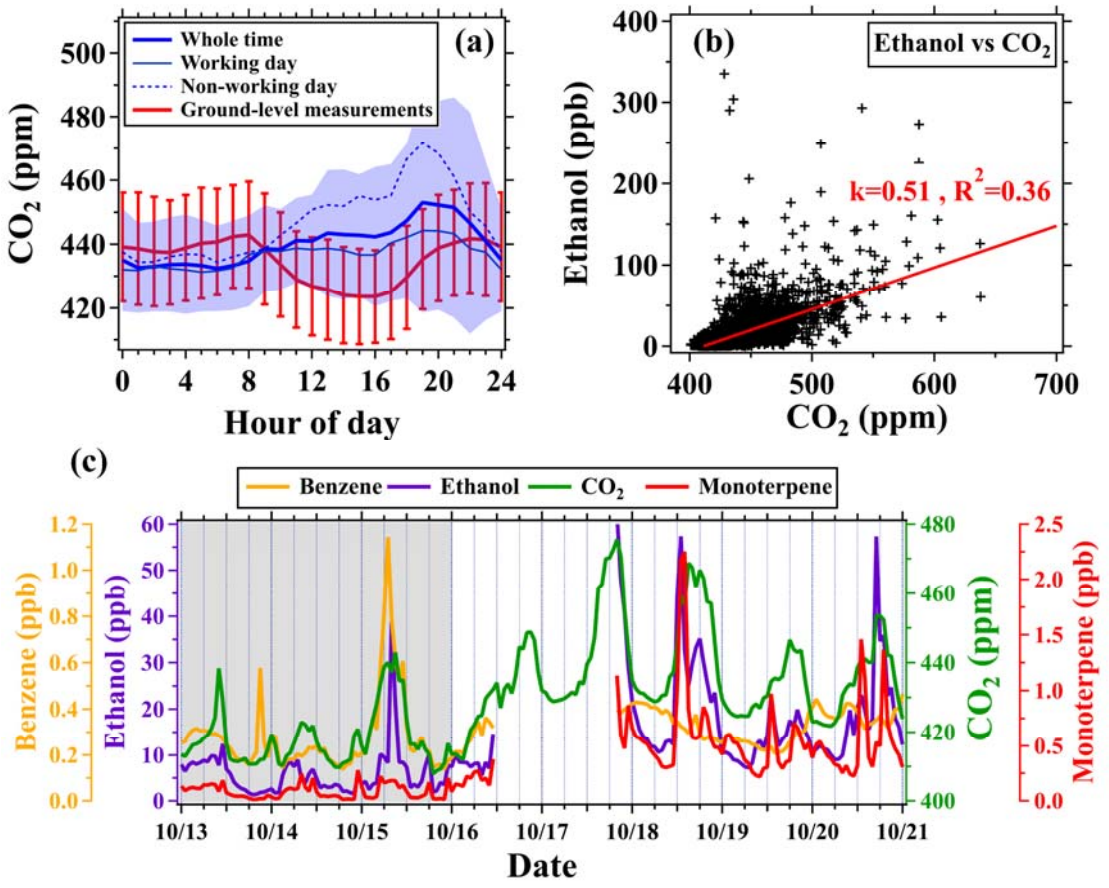

Figure 5. (a) Diurnal variations in CO_2 mixing ratios at 450 m and the ground level, respectively. (b) Scatterplots of 10-min mean mixing ratios of ethanol versus CO_2 measured at 450 m during the CTT campaign.(c) Time series of benzene, ethanol, CO_2, and monoterpene mixing ratios measured at 450 m from October 13 to 21; The grey shaded area indicates the period (October 13–21) when the 450-m platform was closed due to the influence of Typhoon Kompasu.

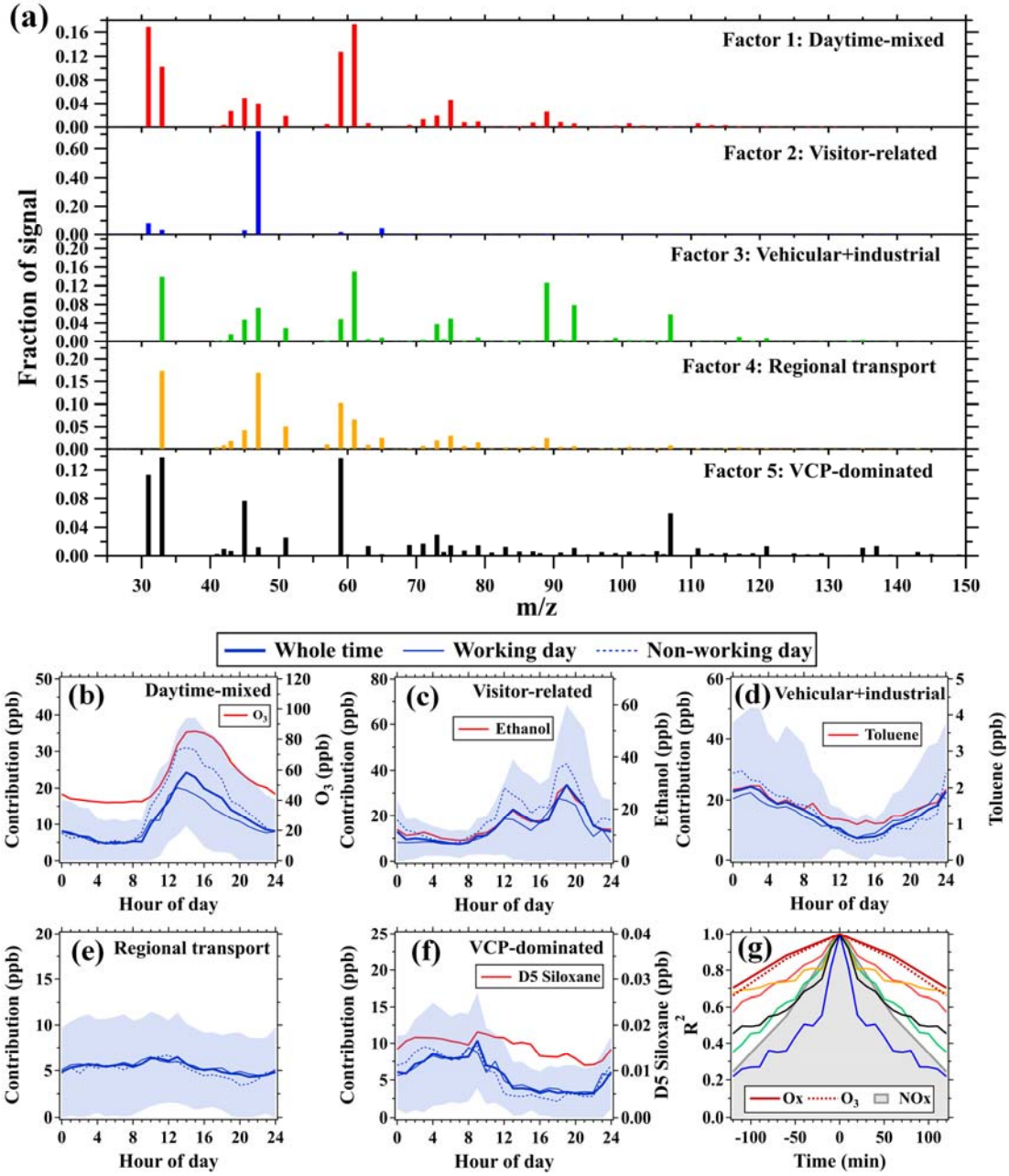

Figure 6. (a) Factor profiles (m/z≤150) of the five PMF factors; Factor profiles with a full range of the mass spectra are provided in Figure S7. (b-f) Average diurnal profiles of the five PMF factors and source tracers. (g) Autocorrelation of the time series of the five PMF factors along with Ox, ozone, and NOx mixing ratios at 488 m; Colors of lines are consistent with the five factors in panel (a).

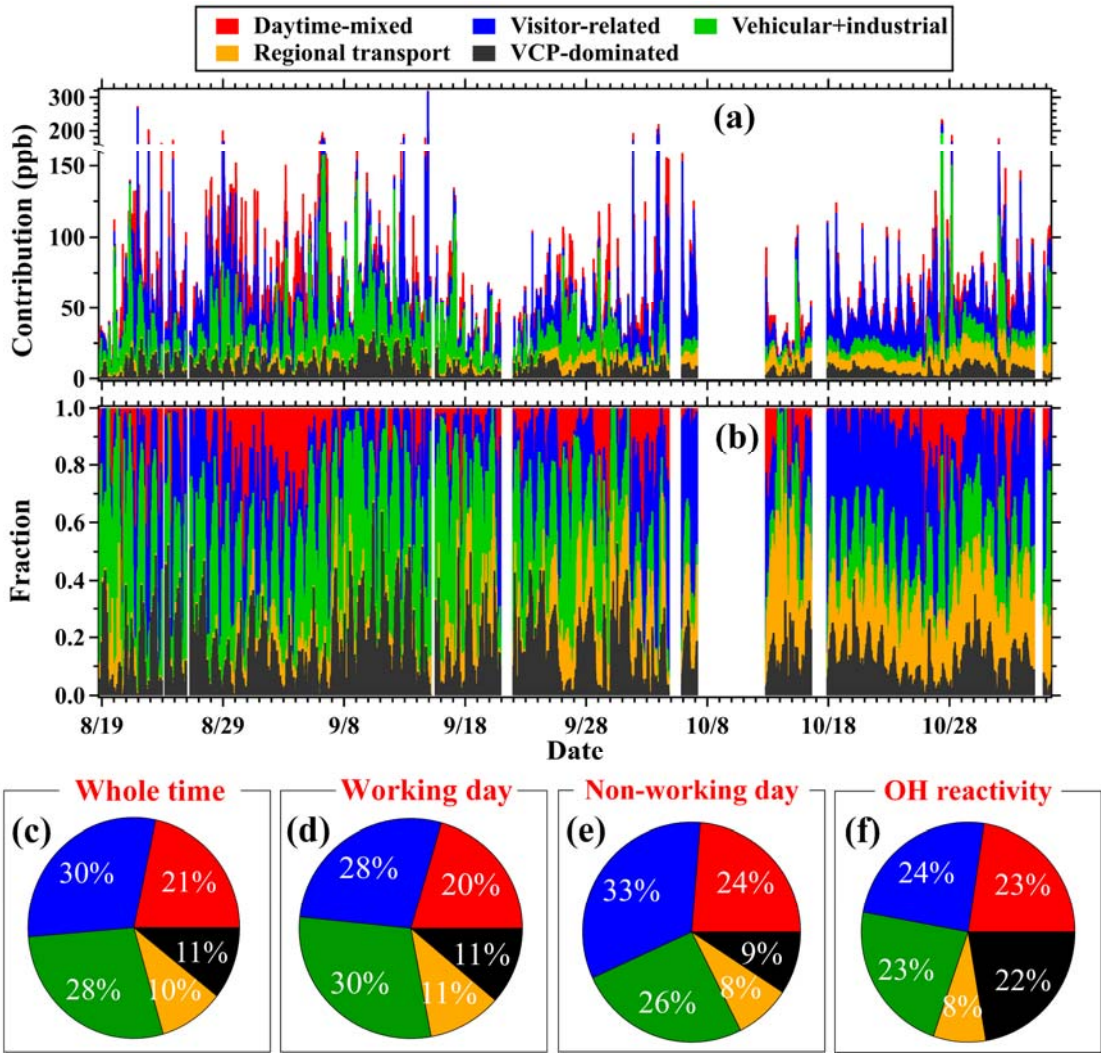

Figure 7. (a-b) Stacked time series of factor fractions and factor contributions for the PMF analysis. (c-e) Average contribution percentages of the five PMF factors to (c-e) the total VOCs concentrations in the whole time, working days, and non-working days and (f) the total OH reactivities during the CTT campaign. In panel (d), only the VOCs species that have known reaction rate constants with OH radical (Table S1) were used.

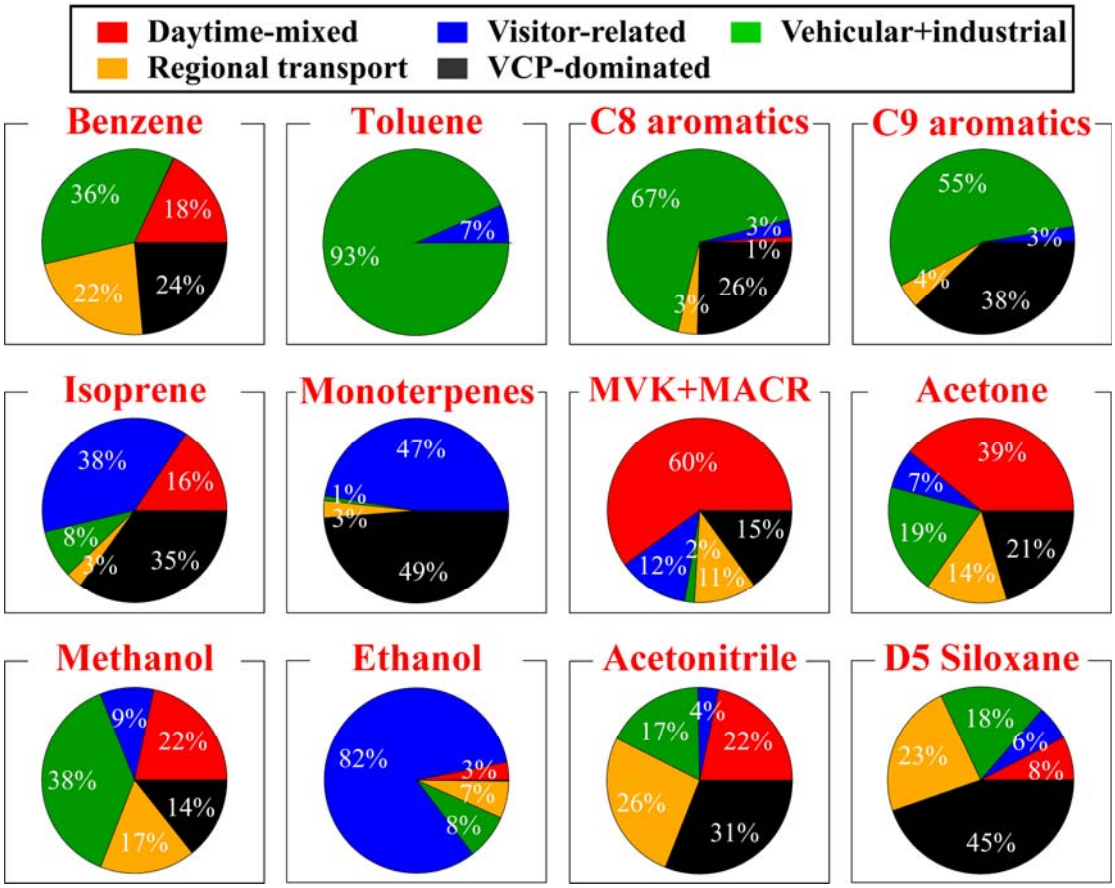

Figure 8. (a) Average contribution percentages of the five PMF factors to concentrations of the 9 selected VOC species during the CTT campaign.

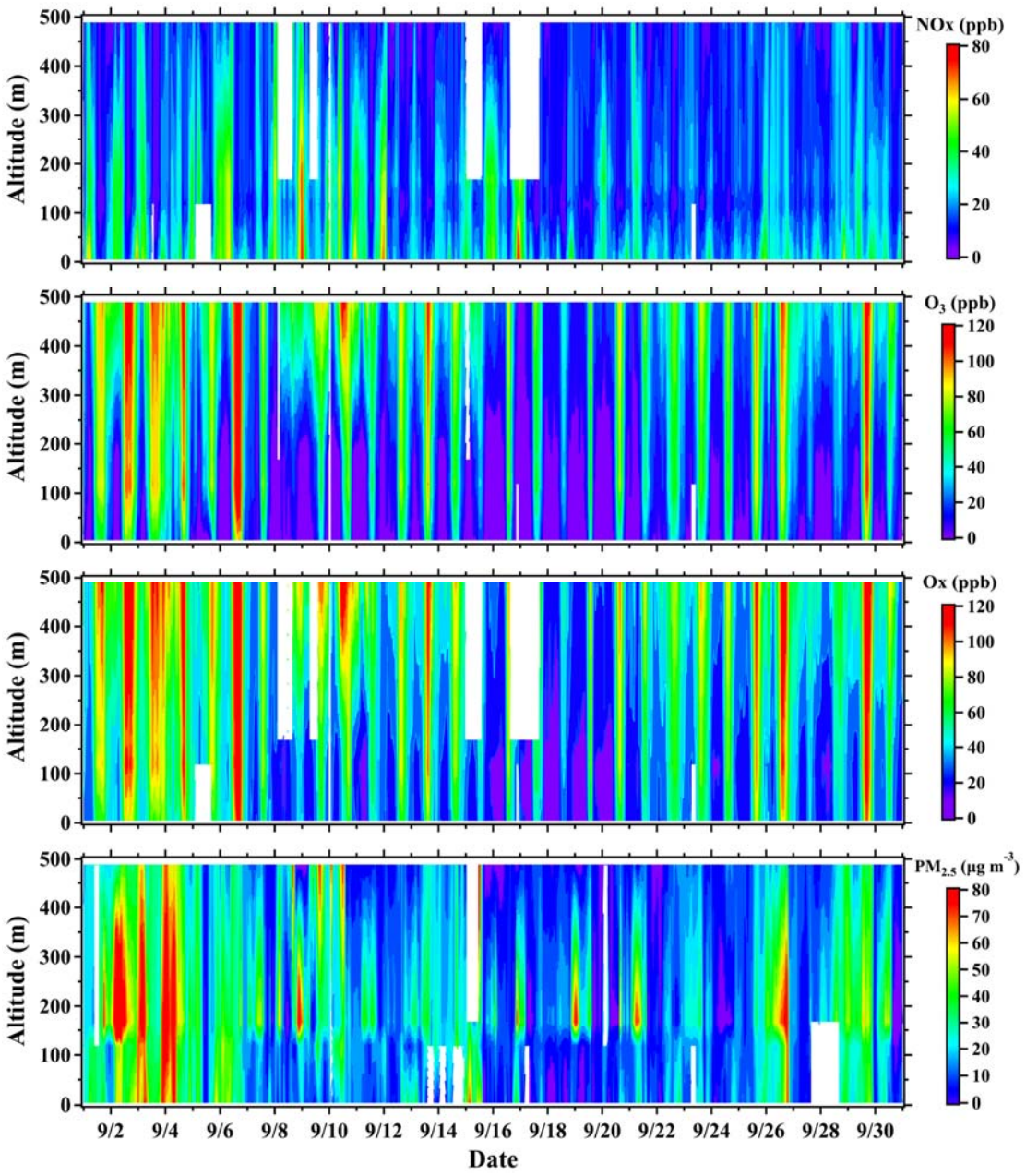

Figure 9. Time series of vertical profiles for O_3, NOx, Ox (O_3+NO_2), and $PM_{2.5}$ concentrations in September during the CTT campaign. The contour plots are made using the measurements from the four CTT sites (5 m, 118 m, 168 m, and 488 m).

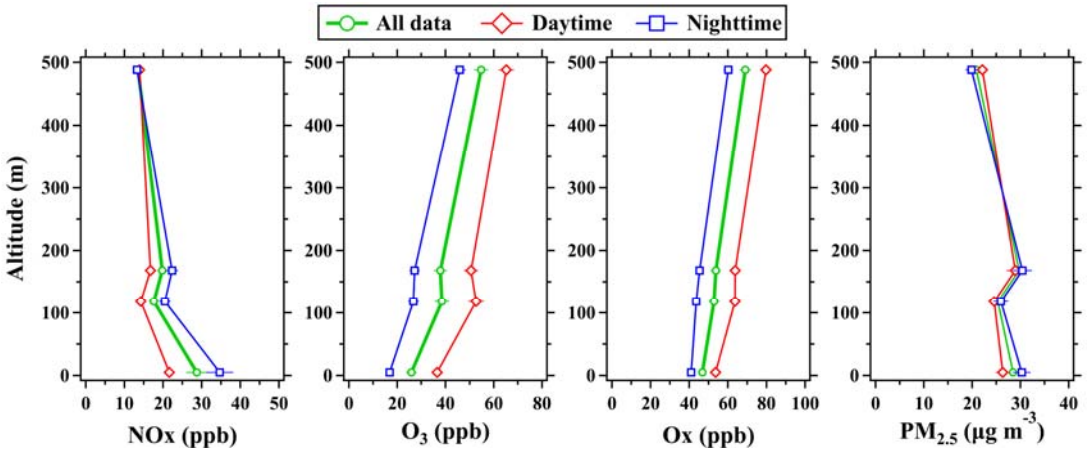

Figure 10. Average vertical profiles of O_3, NOx, Ox (O_3+NO_2), and $PM_{2.5}$ concentrations (mean ± 0.1 standard deviations) measured at the four CTT sites (5 m, 118 m, 168 m, 488 m) during the campaign. Daytime refers to the time between LT 08:00–18:00; nighttime refers to the time between LT 19:00–05:00.

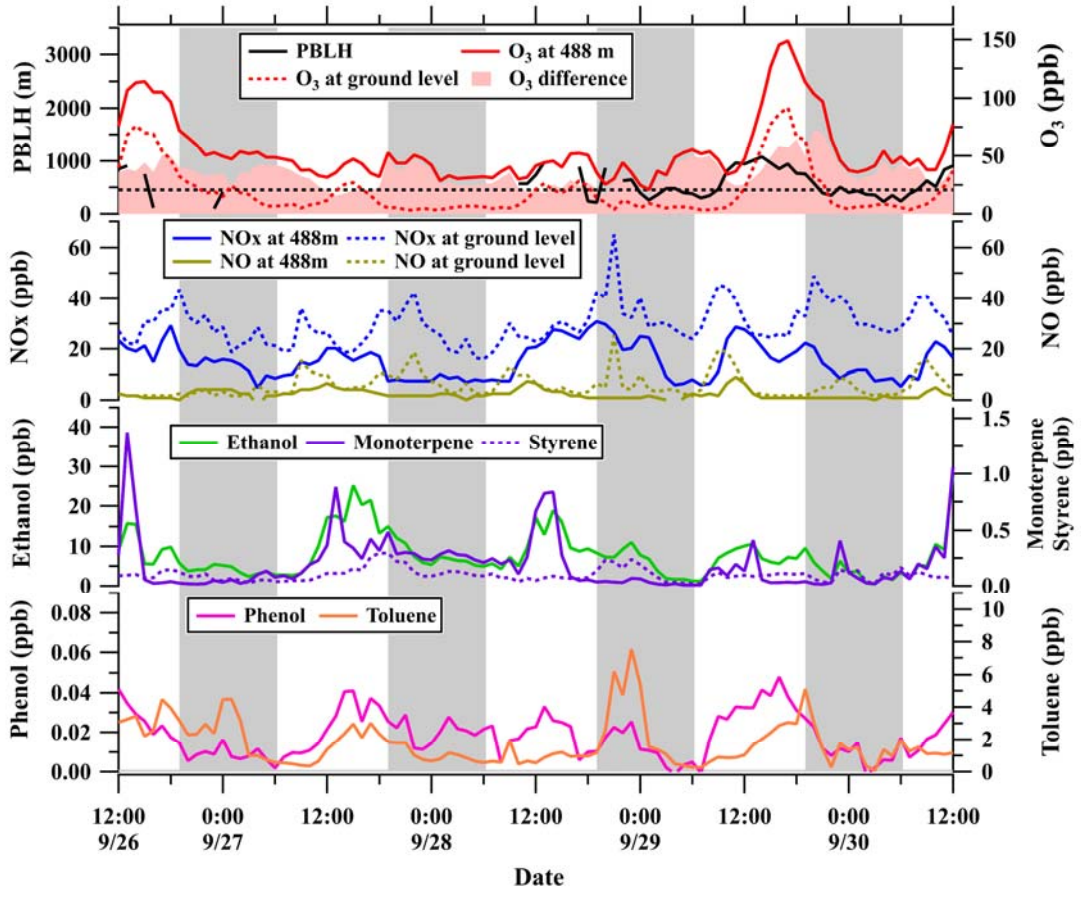

Figure 11. Time series of O_3, NOx, NO, ethanol, monoterpene, styrene, phenol, and toluene mixing ratios along with planetary boundary layer height (PBLH) during September 26–30. O_3 difference refers to the differences in ozone mixing ratios between 488 m and 5 m. Grey shaded areas indicate nighttime periods (LT 19:00–05:00).